2-1

CR-114583
Available to the Public

SURVEY OF NEEDS AND CAPABILITIES FOR WIND TUNNEL TESTING OF DYNAMIC STABILITY OF AIRCRAFT AT HIGH ANGLES OF ATTACK

by

K. J. Orlik-Rückemann

NASA Contract No. NAS2-7279

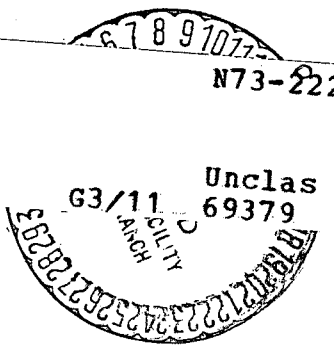

1973

TABLE OF CONTENTS

		Page
	Symbols	4
1.	Introduction	6
2.	Needs for dynamic stability information	8
	2.1 Space shuttle	10
	2.2 High performance military aircraft	20
	2.3 STOL transport aircraft	33
	2.4 Summary of needs for testing capabilities	36
3.	Experimental capabilities available	38
	3.1 Questionnaire	43
	3.2 Wind tunnels included in the survey	44
	3.3 Facilities for measuring pitch and yaw damping	45
	3.4 Facilities for measuring derivatives due to rolling	50
	3.5 Facilities for measuring other dynamic derivatives	54
	3.6 New facilities for measuring dynamic derivatives	56
4.	Needs versus existing capabilities	64
5.	Summary and recommendations	66
6.	Acknowledgment	72
	References	73

TABLE OF CONTENTS (concluded)

		Page
Appendix 1:	Organizations and persons visited	83
Appendix 2:	Questionnaire on dynamic stability test equipment	85
Appendix 3:	Organizations covered by present survey	87
Appendix 4:	Returned questionnaire - JPL	89
Appendix 5:	Returned questionnaire - NOL	91
Appendix 6:	Dynamic stability balances - AEDC	92
Appendix 7:	Dynamic stability balances - NASA-LRC-HS	93
Table 1:	Hypervelocity and hypersonic wind tunnels equipped for dynamic stability experiments	94
Table 2:	Supersonic wind tunnels equipped for dynamic stability experiments	96
Table 3:	Transonic wind tunnels equipped for dynamic stability experiments	98
Table 4:	Subsonic wind tunnels equipped for dynamic stability experiments	100
Table 5:	Facilities for measuring pitch and yaw damping derivatives	101
Table 6:	Facilities for measuring derivatives due to rolling	108
Table 7:	Facilities for measuring other dynamic derivatives	112
Table 8:	Needs versus capabilities	114
Figures 1 - 11		116-126

SYMBOLS

All dynamic stability data are referred to the body axis system.

b	wing span
$\bar{c}$	mean aerodynamic chord
F_A	axial force
F_N	normal force
F_Y	force along Y-axis
M	Mach number
M_X	rolling moment
M_Y	pitching moment
M_Z	yawing moment
p	rolling angular velocity
q	pitching angular velocity
q_∞	free-stream dynamic pressure
r	yawing angular velocity
S	wing surface area
V	free-stream velocity
X,Y,Z	body reference axes
α	angle of attack,
$\dot{\alpha}$	rate of change of angle of attack
β	angle of sideslip
$\dot{\beta}$	rate of change of angle of sideslip
ρ	air density
ϕ	angle of roll
Ω	rate of rotation in spin

SYMBOLS (concluded)

$$C_m = \frac{M_Y}{q_\infty S\bar{c}} \qquad C_N = \frac{F_N}{q_\infty S} \qquad C_A = \frac{F_A}{q_\infty S}$$

$$C_{m_q} = \frac{\partial C_m}{\partial \frac{q\bar{c}}{2V}} \qquad C_{N_q} = \frac{\partial C_N}{\partial \frac{q\bar{c}}{2V}} \qquad C_{A_q} = \frac{\partial C_A}{\partial \frac{q\bar{c}}{2V}}$$

$$C_{m_{\dot{\alpha}}} = \frac{\partial C_m}{\partial \frac{\dot{\alpha}\bar{c}}{2V}} \qquad C_{N_{\dot{\alpha}}} = \frac{\partial C_N}{\partial \frac{\dot{\alpha}\bar{c}}{2V}} \qquad C_{A_{\dot{\alpha}}} = \frac{\partial C_A}{\partial \frac{\dot{\alpha}\bar{c}}{2V}}$$

$$C_\ell = \frac{M_X}{q_\infty Sb} \qquad C_n = \frac{M_Z}{q_\infty Sb} \qquad C_Y = \frac{F_Y}{q_\infty S}$$

$$C_{\ell_p} = \frac{\partial C_\ell}{\partial \frac{pb}{2V}} \qquad C_{n_p} = \frac{\partial C_n}{\partial \frac{pb}{2V}} \qquad C_{Y_p} = \frac{\partial C_Y}{\partial \frac{pb}{2V}}$$

$$C_{\ell_r} = \frac{\partial C_\ell}{\frac{rb}{2V}} \qquad C_{n_r} = \frac{\partial C_n}{\partial \frac{rb}{2V}} \qquad C_{Y_r} = \frac{\partial C_Y}{\partial \frac{rb}{2V}}$$

$$C_{\ell_{\dot{\beta}}} = \frac{\partial C_\ell}{\partial \frac{\dot{\beta}b}{2V}} \qquad C_{n_{\dot{\beta}}} = \frac{\partial C_n}{\partial \frac{\dot{\beta}b}{2V}} \qquad C_{Y_{\dot{\beta}}} = \frac{\partial C_Y}{\partial \frac{\dot{\beta}b}{2V}}$$

$$C_{\ell_q} = \frac{\partial C_\ell}{\partial \frac{q\bar{c}}{2V}} \qquad C_{n_q} = \frac{\partial C_n}{\partial \frac{q\bar{c}}{2V}} \qquad C_{Y_q} = \frac{\partial C_Y}{\partial \frac{q\bar{c}}{2V}}$$

1. INTRODUCTION

Since the advent of high speed aircraft flying at high angles of attack, such as exemplified by the space shuttle or by the high performance modern military aircraft, the dynamic stability information, considered of rather lesser importance for a number of years, is again becoming an object of relatively high interest. The reason is obvious: at low angles of attack most of the dynamic stability parameters were relatively easy to predict analytically, exhibited as a rule only smaller variations with varying flight conditions and, therefore, had only a relatively insignificant or at least a relatively constant effect on the resulting flight characteristics of the aircraft. In many cases it was therefore satisfactory to use, in the flight mechanics analysis, a constant value of a particular dynamic stability parameter, often determined by some simple approximate method of calculation. With the introduction of flight at high angles of attack at high speeds, all that has drastically changed. The dynamic stability parameters are now found to depend strongly on non-linear effects involving phenomena such as separated flows, vortex shedding, etc., and can no longer be calculated using relatively simple linear analytical methods as in the past. In addition, these parameters are known now to sometimes undergo very large changes, perhaps of one or

even two orders of magnitude and often involving a change of sign, as a result of only a minor variation in flow conditions (such as the angle of attack) and therefore can easily become of significant importance for the flight behaviour of the aircraft.

In this report the needs for dynamic stability data are examined for several types of aerospace vehicles which all are characterized by flying at much higher angles of attack than those which were typical of aircraft of the past. Since, at the present time not enough information in this area exists to permit a completely rigid definition of these needs, the discussion must often, of necessity, be based on reasoning and conjectures rather than on hard facts. This is the best that can be done under present circumstances. That something more must be done and that the problem is real enough is best witnessed by accident statistics, such as mentioned in the section on military aircraft.

After examination of needs, a review is performed of the presently available capabilities for wind tunnel testing of dynamic stability of aircraft. The review covers facilities now in existance in the USA and Canada, and includes information about equipment owned by the two governments as well as by industrial and university organizations.

Finally, by comparing the specified needs with the existing capabilities, a set of recommendations is obtained defining the capabilities that are still lacking and indicating ways and means to remedy that situation.

2. NEEDS FOR DYNAMIC STABILITY INFORMATION

This part of the report is based on a series of interviews with representatives of various US government agencies such as:

USAF: Aeronautical Systems Command, WPAFB, Ohio

USN: Naval Air Systems Command, Arlington, Virginia

NASA: Ames Research Center, Moffett Field, California
Manned Spacecraft Center, Houston, Texas
Langley Research Center, Hampton, Virginia.

At each of these agencies one or more meetings were held with the cognizant personnel and informal discussions were carried out without any recordings or detailed notes. A list of persons who participated in these interviews is given in Appendix 1.

Since the comments received were often of a general rather than specific nature and sometimes were even controversial, no attempt was made in the text to attribute any opinions to the individual persons interviewed. Rather,

and in order to present the situation in a manner as clear and as coherent as possible, the material was organized according to the subject matter and not to the source of origin. A large number of documents, partly made available to the author during or after the visits, was also consulted and some of them are given as references. All together the material in this section represents the author's synthesis of all the material made available to him, with an unavoidable sprinkling of his own views.

The three main categories of aerospace vehicles considered during this study are:

1) space shuttle
2) high performance military aircraft
3) STOL transport aircraft.

The only common factor between these vehicles is that their performance envelope contains much higher angles of attack than those employed in the past. Other factors, such as configurations, propulsion systems, lift devices, etc., are quite different for each category. The speed ranges vary all the way from low subsonic to hypersonic. The possible needs for dynamic stability information will be discussed separately for each category.

2.1 Space Shuttle

Of the various aerospace vehicles considered in this study, the space shuttle certainly represents the most significant departure from the flight conditions of a conventional aircraft. A typical reentry trajectory for the delta-wing shuttle orbiter is shown in Fig. 1. The requirement for a high angle of attack ($20^{\circ}<\alpha<40^{\circ}$) at high supersonic and hypersonic speeds is unique. No other existing or planned aerospace vehicle has such a flight envelope and no previous experience of the flight behaviour at such conditions is available. At lower speeds, and particularly after the subsonic transition to low angle-of-attack flight, the shuttle behaves more like many other modern aircraft. In fact, at transonic speeds, its maximum angle of attack is considerably lower than that of a military aircraft under a high performance maneuver and represents therefore a less critical situation.

One of the consequences of flying at a high angle of attack is the flow separation on the leeward side of the orbiter wing. Several possible types of such a flow separation have been identified, including the shock-induced separation and the leading-edge stall (see e.g. Ref.1).

It is also important to remember, that when the angle of attack is in the vicinity of the angle for incipient stall, even a small perturbation in the flight attitude can cause a sudden large change in the aerodynamic characteristics of the vehicle. As the result, the stability derivatives at high angle of attack not only are extremely difficult to predict analytically but also can frequently be subject to sudden and large variations, sometimes involving changes by orders of magnitude.

In order to gain some understanding of the relative importance of the various stability derivatives when employed in the flight mechanics analysis of the shuttle orbiter, sensitivity studies have been conducted by some NASA centers using a nominal set of derivatives in the equation of motion and investigating the effect of varying the value of an individual derivative. As the result, the following dynamic stability derivatives were identified as having a significant effect on the flight behaviour of the orbiter:

(a) in the subsonic range: C_{mq}, $C_{\ell p}$, C_{nr}, C_{np}, $C_{\ell r}$, $C_{m\dot{\alpha}}$

(b) in the transonic range: C_{mq}, $C_{\ell p}$, C_{nr}, C_{np}

(c) in the supersonic range: C_{mq}, $C_{\ell p}$.

In addition, the following derivatives were indicated

as having a "second order effect" on the flight behaviour of the orbiter (i.e. an effect of the order of 5-10 percent on some resulting characteristic of the orbiter motion):

(a) in the subsonic range: $C_{n\dot{\beta}}$, C_{Yp}, C_{Yr}

(b) in the transonic range: $C_{\ell r}$, $C_{m\dot{\alpha}}$, $C_{n\dot{\beta}}$

(c) in the supersonic range: C_{nr}, C_{np}, $C_{\ell r}$.

It should be noted, however, that in all cases known to the present author, the aforementioned sensitivity studies were carried out using assumptions representative of the low angle-of-attack case. Specifically, the nominal set of derivatives was based on calculations typical of unseparated flow conditions, and the individual derivatives were varied by 50-100 percent rather than by orders of magnitude. That was so, of course, because no other information was available. Also, it should be recognized that a flow separation phenomenon at high angle of attack, if properly accounted for, may cause a sudden variation not only in one but in a whole set of derivatives, at the same time. Thus the aforementioned list of derivatives must be considered as only representative of a <u>minimum</u> set of requirements, mainly pertaining to the low angle-of-attack flight conditions.

Since no previous experience exists of the high speed flight at high angles of attack, no assessment can be made

at the present time of the relative significance of the various derivatives on a flight mechanics analysis of the shuttle flight. The foregoing remarks, however, indicate that flow phenomena at high angles of attack differ distinctly from those prevailing at lower angles of attack, and that sudden and possibly very large variations in the value of the different aerodynamic parameters may be expected. It may further be inferred that, because of the various time-lag effects that usually are associated with separated flows, the unsteady aerodynamic effects may be particularly large, affecting the dynamic stability derivatives to an even higher degree than the purely static aerodynamic parameters. All that, however, still does not necessarily clarify whether such a large expected variation in the values of the individual dynamic derivatives must also have a large effect on the flight behaviour of the shuttle orbiter.

To assess the significance of the various derivatives in this regard, another sensitivity study is required, based on a realistic (high angle of attack) set of stability derivatives, and realistic (very large and in combinations rather than individual) variations of these derivatives. To obtain the required input information for such a study, a complete set of static as well as dynamic stability

derivatives is therefore needed at least for one typical configuration of the shuttle and for those speed ranges where flight at high angles of attack is required. This means primarily at supersonic speeds and, to some extent, also at transonic speeds (where, however, the angles of attack may be considerably smaller). Since the possibility of an analytical determination of these derivatives under the flow conditions of interest appear, to say the least, somewhat questionable (although quasi-steady, semi-empirical techniques have been employed - as in Ref. 1 - to obtain qualitative descriptions of the effects involved), the only reliable course appears to be through a suitable series of experiments. Since flow separation effects usually are a strong function of viscous effects, these experiments have to be conducted at properly simulated Reynolds numbers (see Fig. 1). Of the different experimental facilities that could be available for such studies, wind tunnels appear to offer most promise, both from the point of view of Reynolds number simulation, accuracy of experiments and economy.

Since the hypersonic portion of the orbiter reentry takes place at high altitudes (Fig. 1), both the dynamic pressure and the product (ρ.V) are relatively low and the dynamic derivatives may therefore be expected to be of

lesser importance than at lower altitudes. Hence it is probably sufficient to only investigate the most important dynamic derivatives, such as C_{mq} and $C_{\ell p}$, at hypersonic speeds.

Although Fig. 1 indicates a maximum angle of attack of less than 40°, higher angles may be envisaged for reentry maneuvers designed for lower-than-maximum cross-range. In the high supersonic range, therefore, dynamic derivatives should be investigated at angles of attack up to 50° or even 55°.

So far in this paragraph derivatives C_{mq} and $C_{m\dot{\alpha}}$ have been treated separately. Although at subsonic speeds this appears desirable, at higher speeds it may, in general, be acceptable to determine only the sum of these two derivatives experimentally (which is the form in which results are obtained from oscillatory experiments about a fixed axis, such as usually performed in wind tunnels) and to separate them by some semi-empirical means. Again however, at higher angles of attack, no previous experience for such a procedure exists and it seems advisable, at least at transonic and low supersonic speeds, to determine both derivatives experimentally at least for a limited number of cases. Similar comments apply to derivative $C_{n\dot{\beta}}$ and its

appearance in expressions such as ($C_{nr} - C_{n\dot{\beta}}\cos\alpha$) and ($C_{np} + C_{n\dot{\beta}}\sin\alpha$). Although all the dynamic derivatives with respect to $\dot{\beta}$ are to some extent sensitive to the lag in flow separation and flow reattachment which may occur on highly swept wings at high angles of attack, derivatives $C_{\ell\dot{\beta}}$ and $C_{Y\dot{\beta}}$ are believed to be of lesser significance than $C_{m\dot{\alpha}}$ and $C_{n\dot{\beta}}$ and their contribution to expressions such as ($C_{\ell p} + C_{\ell\dot{\beta}}\sin\alpha$) or ($C_{\ell r} - C_{\ell\dot{\beta}}\cos\alpha$) probably may be neglected.

In view of all the above remarks, experimental information on the following dynamic derivatives may be considered desirable for the orbiter reentry flight (with an asterisk denoting those derivatives, that initially may be needed for one configuration and a few flight conditions only):

(a) subsonic speeds, $-5^\circ<\alpha<20^\circ$:

C_{mq}, $C_{\ell p}$, C_{nr}, C_{np}, $C_{\ell r}$, $C_{m\dot{\alpha}}$, $C_{n\dot{\beta}}$

(b) transonic speeds, $M \leq 2$, $0^\circ<\alpha<20^\circ$:

C_{mq}, $C_{\ell p}$, C_{nr}, C_{np}, $C_{\ell r}$, $C^*_{m\dot{\alpha}}$, $C^*_{n\dot{\beta}}$

(c) supersonic speeds, $2<M<7$, $0^\circ<\alpha<50^\circ$:

C_{mq}, $C_{\ell p}$, C_{nr}, C^*_{np}, $C^*_{\ell r}$

(d) hypersonic speeds, $M > 7$, $10^\circ<\alpha<55^\circ$:

C_{mq}, $C_{\ell p}$, C_{nr}

For the purposes of this list the rotary derivatives such as C_{nr} may be replaced by the corresponding "fixed-axis" derivatives such as $(C_{nr} - C_{n\dot{\beta}}\cos\alpha)$.

As pointed out before, it is highly essential that the derivatives be measured at a high enough Reynolds number (see Fig. 1) to properly simulate the viscous flow around the orbiter and in particular the separated and reattached flows at higher angles of attack.

In addition to the above strong requirements for the dynamic stability derivatives for the orbiter during its reentry phase, there is also a certain need for this type of information for the launch configuration of the shuttle. However, probably only the most important derivatives, such as C_{mq}, $C_{\ell p}$, C_{nr}, are required, since the flight behaviour of the launch configuration can, in general, be controlled very well by vectoring the thrust of the booster and orbiter engines during the ascent. Some special problems, which may have a very large (orders of magnitude) effect on some of these important derivatives, may still have to be looked into. One example of such special problems is the possible pulsation of the rocket jet exhaust and its effect on the flow field around the vehicle and, therefore, on its dynamic stability characteristics. Such a pulsation

may typically reach amplitudes of the order of 10 percent or so of the pertinent dynamic pressure (at Mach 1.5) and may be important at transonic and supersonic speeds, where the exhaust plume, due to the low density of the atmosphere which surrounds the vehicle at these speeds, is very large. This effect may be expected to be particularly significant for exhaust pulsation frequencies which are close to the oscillatory frequency of the vehicle.

Another example of a special problem pertains to the flight dynamics of an abort separation maneuver. As was shown in Refs. 2 and 3 for the previously considered fully reusable version of the shuttle (delta wing orbiter and canard booster), under certain - rather special - separation conditions, the two vehicles could find themselves for a short period of time in a situation where they performed oscillation in pitch in near-resonance with each other; in such a situation and depending on the phase shift between the two motions, the damping-in-pitch derivative could change sign and also could vary by one to two orders of magnitude, which - in turn - could have significant effects on the trajectory of the orbiter during abort separation. Whether such a condition may also arise during an abort separation of the currently envisaged shuttle orbiter from its liquid-oxygen tank is at present not known.

The above two special problems are examples of situations which may cause difficulties if not recognized in advance, but which can probably be entirely avoided if sufficient information is available early enough to influence the proper formulation of the design and/or operation requirements. They are also examples of situations where the presence of resonance or near-resonance between two physical phenomena or motions may dramatically affect the dynamic stability derivatives without necessarily similarly affecting the static aerodynamic characteristics (as shown in Ref. 2). It is important that such situations be identified early, and - if possible - avoided.

At the present time the only dynamic stability information that so far has been obtained for the shuttle consists of some experimental data on damping-in-pitch at low supersonic speeds and at low angles of attack, contained in Refs. 2 and 4. In view of the remarks of the present section, this appears to be totally inadequate. More dynamic stability work is therefore badly needed. In this connection it should also be kept in mind that any such information obtained now for the present version of the shuttle may in the future also find applications to more advanced aerospace systems, such as a long range high speed transportation system using boosted gliders, a second

generation (presumably fully reusable) two-stage shuttle, as well as a possible future single-stage-to-orbit shuttle. Also, although only some of the results obtained for the present shuttle may find direct application to a possible future hypersonic transport (which most often is envisaged as a slender vehicle flying at low angles of attack), the experimental techniques developed for the shuttle may very well be used also for that project.

2.2 High Performance Military Aircraft

It is well known that many of the high performance military aircraft have flying characteristics that become rather unsatisfactory when the aircraft is performing maneuvers near or above the stall or during the spin motion. The loss of control that often results has been named as the direct cause of a large number of fatal accidents. The seriousness of the situation can best be appreciated by recognizing the fact that, in addition to a large loss in human lives, the order of magnitude of the average material losses caused by such accidents is sometimes estimated at the staggering amount of 100 million dollars a year.

At the present time the flying characteristics of an aircraft during the incipient, developed or recovery

phases of the spinning motion are not completely predictable by analytical means. During a number of studies conducted with now existing and fully operational aircraft it has been virtually impossible to obtain a true match between the analytical predictions and the full-scale results. Two of the possible reasons for this situation are: (a) the possible inadequacy of the present mathematical model of analysis and (b) the almost total lack of aerodynamic data that would apply to a full-scale aircraft during the various phases of the spinning motion.

The mathematical model used for this type of analysis is normally based on equations of motion that are similar to the classical small perturbation approach to aircraft dynamics. Thus the aerodynamic information is usually expressed in the form of stability derivatives and based on the steady and oscillatory types of data, where perhaps stepwise variations and the use of indicial functions, such as discussed in Ref. 5, would be more representative of the actual flight conditions, at least during the departure phase of the spinning motion. A certain amount of nonlinearities in the data has often to be accepted, even if this introduces uncertainty in the appropriatness of the linear superposition of the separate effects of rotation

around the three axes and effects of the various control deflections, that is almost always used in the analysis. A nonlinear aerodynamic moment formulation, of the type that possibly could be extended to analyze the developed phase of the spinning motion, has recently been suggested (Ref. 6).

The Mach number and the angle-of-attack ranges, for which the aerodynamic data are required for a modern military high-performance aircraft under the various phases of the spinning motion, may be assumed to be as follows:

$\alpha \leq 50^{\circ}$: $0.4 < M < 1.5$ (2.0)*

$\alpha \leq 90^{\circ}$: $M \leq 0.4$

It should be noted that at high angle of attack compressibility effects may be important at Mach numbers as low as 0.4. In addition, as discussed in the previous paragraph and also in numerous references, such as Ref. 7 and 8, the aerodynamic data should be representative of the full-scale Reynolds number for the actual flight condition. This is of particular importance for modern aircraft, where the body contributes a significant portion of the aerodynamic forces and moments; especially the flow around the forebody of the

---

* For example, during recent spin prevention tests in Calverton, N.Y., Grumman has flown its F-14 fighter, without the weapons system, at 6.5g at Mach 2.05 at 42,000 ft.

aircraft (which may be characterized by asymmetrical vortex shedding, see Ref. 9) is known to be very sensitive to Reynolds number effects. Although efforts have often been made to simulate the flow conditions that are typical for higher (supercritical) Reynolds numbers using artificial flow-disturbance or flow-tripping devices such as grit strips and strakes, such procedures have to be applied with great care, since their effects usually depend strongly on the particular configuration and flow conditions and often require a verification by means of a separate static wind tunnel investigation. At conditions close to stall, when even minor changes in the angle of attack may cause large variations in the various aerodynamic coefficients and derivatives (as illustrated, at low speeds, by some of the results in Refs. 9-12), there hardly seems to be any foolproof alternative to simulating the flow conditions at high Reynolds number other than by duplicating the Reynolds number itself. This may be specially important for dynamic stability derivatives because of their dependence on the unsteady aerodynamic phenomena such as viscous time lags, which are often associated with partly separated flows (see paragraph 2.1). At the present time only a very limited amount of such aerodynamic information can usually be made available for the combination of Mach number, Reynolds number and angle of attack that is

representative of the various phases of spinning motion; if available at all, such information applies to already existing aircraft. For aircraft still in the design stage, no reliable dynamic stability information, based on the simulation of all three of the abovementioned parameters, can be obtained, due to the lack of necessary experimental capabilities. Instead, such information is at the present time calculated analytically, using approximate methods of analysis such as the "strip hypothesis" described in Ref. 7, or else is estimated on the basis of experimental data for a similar (but, of course, not the same) configuration, for which full-scale flight-test data already may be available. However due to the expected great sensitivity, in the (stall/post-stall/spin)-region, of the dynamic stability parameters to even minor variations in aircraft configuration or flow conditions, these procedures cannot be expected to yield fully satisfactory results at those critical flight attitudes. In addition, although new methods such as that of maximum likelihood estimation, Refs. 13 and 14, for extracting derivatives from flight-test data, are constantly being developed, their accuracy, especially at high angles of attack and with regard to other than the most commonly employed dynamic derivatives, cannot yet be considered adequate. Hence it must be concluded that at the present time no completely satisfactory means exist of obtaining

all the dynamic derivatives that may be important for a satisfactory prediction of full-scale flight at high angles of attack, such as during the (stall/post-stall/spin)-maneuvers.

Although it is rather difficult to be certain which of the two abovementioned possible sources of error is more important, it appears that the lack of aerodynamic data at properly simulated flight conditions may be more significant than the approximations and omissions in the analysis of motion. A logical first step of an attempt to remedy the present unsatisfactory situation regarding the accuracy of predictions of the (stall/post-stall/spin)-maneuvers would therefore be an all-out effort to obtain a satisfactory set of representative experimental data for at least one existing modern aircraft and to compare the resulting analytical predictions (using present methods of analysis) with the observed full-scale flight characteristics, to assess the efficiency of such an improved approach.

Since the same lack of proper Reynolds number and high angle-of-attack simulation already has been recognized for certain types of aerodynamic data such as those pertaining to the static stability and drag characteristics of an aircraft, wind tunnels for all speed ranges (and especially for transonic speeds) with high Reynolds number

simulation capabilities are rapidly becoming available or are being proposed. What is still lacking is the capability, in these wind tunnels, for measuring all the necessary dynamic stability derivatives (if the present methods of analysis will continue to be used) or for studying the spinning motion more directly (as can be done by employing devices such as rotary balances, to be discussed later in this report).

Up to now the dynamic stability experiments, if at all included in the wind tunnel studies, have usually been scheduled at such a late stage in the development of a new aircraft, that any real chance of seriously affecting the design was practically non-existent. If it can be shown that with properly obtained static and dynamic aerodynamic data the stall and spin characteristics of an aircraft can be predicted successfully, it would become necessary to schedule this type of testing at an early stage of the preliminary design. Even if the resulting design improvements could avert only one fatality due to out-of-control accidents, the extra cost and time for the thereby increased wind tunnel testing would be fully justified.

It remains to discuss the relative significance of the various dynamic stability derivatives and to list those,

for the measurement of which proper wind tunnel equipment should be available. As in the case of the shuttle orbiter, and mostly for the same reasons, no truly representative sensitivity study seems to exist at the present time. For instance in Refs. 15 and 16, which describe the most detailed such study known to the present author, a "base value", typical of low angle-of-attack flight conditions for a variety of operational aircraft, was assigned to each dynamic derivative and the effect on spin motion of varying this derivative from zero to twice the base value was investigated. For such a variation, which was considered for several types of spin (two values of an inertia parameter and two values of a parameter associated with yawing moment induced by deflection of the lateral control), the following dynamic derivatives were found, under certain conditions, to have a "significant effect" (indicating that a large change in some spin characteristic was evident and is of academic interest) or even an "appreciable effect" (indicating that the over-all nature of the spin was changed and could be easily recognized by a pilot):

$$C_{mq},\ C_{\ell p},\ C_{nr},\ C_{\ell r}.$$

The "appreciable" rating was usually associated with the zero value of the particular derivative. The effects of derivative C_{np} and the acceleration derivatives $C_{m\dot{\alpha}}$, $C_{n\dot{\beta}}$

and $C_{\ell\dot{\beta}}$ were under all conditions found to be "insignificant" (indicating that no effects or only very slight effects were noted).

However it is known now, from studies such as the previously quoted Refs. 9-12, that the dynamic derivatives at high angles of attack may become not only twice but as much as 10-20 times larger than their low angle-of-attack values; in addition a change in sign (including, of course, a zero crossing) may also be involved. Thus the results of the aforementioned sensitivity study must be considered as defining only the very minimum set of derivatives important for a spin analysis; a new sensitivity study, which would take into account the very large variations in the dynamic derivatives at high angles of attack and which also would examine the effect of a simultaneous variation of several of these derivatives, would probably result in an increase in the number of important derivatives. Such a new sensitivity study appears badly overdue.

An added complication arises due to the fact that some of the dynamic derivatives (and especially the damping-in-yaw derivative) display a strong dependence not only on the angle of attack but also on the rate of rotation in a spin (Refs. 10 and 12). This effect would have to be included for a meaningful analysis.

The importance of the three damping derivatives, C_{mq}, $C_{\ell p}$ and C_{nr}, is established beyond any doubt. Both early and present investigators of flight and control characteristics of an aircraft agree unanimously on that point. More recently, however, we can also find direct references regarding the need for some of the other derivatives, some of which were considered earlier as completely insignificant. For instance in the impressive report "Background information and user guide for MIL-F-8785B(ASG)-Military Specification-Flying Qualities of Piloted Airplanes" (Ref. 17) we find in the paragraph on lateral-directional flying qualities, on p. 179, a discussion of the roll-sideslip coupling requirements as related to the dynamic controllability problem. A statement is made that "for dynamic controllability the primed rate derivatives $L'_{\dot\beta}$, $N'_{\dot\beta}$, L'_r, N'_r, L'_p, N'_p and the bank angle side force term, q/V, must also be considered". The above "primed derivatives" are expressions that contain various moments and products of inertia as well as the aerodynamic derivatives

$$C_{\ell\dot\beta},\ C_{n\dot\beta},\ C_{\ell r},\ C_{nr},\ C_{\ell p} \text{ and } C_{np}.$$

In a report dealing with "An in-flight investigation of lateral-directional dynamics for the landing approach" (Ref. 18) we find, similarly, that "the yaw coupling

effects of $N'_{\delta_{Aw}}/L'_{\delta_{Aw}}$ and N'_p are important factors in the pilot's control of bank angle" (page 10) and that "...for fixed values of..., the value of N'_p strongly influences the position of the ϕ/δ_{Aw} numerator zero..." (page 25) as well as that "the optimum value of $N'_{\delta_{As}}/L'_{\delta_{As}}$ for a configuration is primarily a function of the yaw-due-to-roll rate parameter, N'_p" (page 25). In Ref. 19, which contains an "Evaluation of lateral-directional handling qualities and roll-sideslip coupling of fighter class airplanes", a special investigation of the effects of derivative N'_p is made and we find, for example, that "to satisfy the roll-sideslip requirements of MIL-F-8785B(ASG) at low Dutch roll frequency demands very precise control over coupling derivatives such as (N'_p - q/V) and $N'_{\delta_{As}}$. Both these derivatives are notoriously difficult to identify and equally difficult for the designer to control. In addition, consideration must be given to yawing moment due to yaw rate, N'_r." (page 36). Again, the primed derivative N'_p contains mainly the effect of

C_{np}, with a smaller contribution from $C_{\ell p}$,

and the primed derivative N'_r consists mainly of

C_{nr}, with a smaller contribution from $C_{\ell r}$.

It may also be of interest to note that among the aerodynamic data that a contractor is required to submit in his Stability and Control Analysis Report and that are intended for use as input data for computer studies, for fixed and moving base simulator studies, and for the prediction of aircraft flying qualities over the flight envelope of the aircraft, the following dynamic stability derivatives are listed:

C_{mq}, $C_{m\dot{\alpha}}$, $C_{\ell p}$, $C_{\ell r}$, $C_{\ell\dot{\beta}}$, C_{nr}, C_{np}, $C_{n\dot{\beta}}$, C_{Yp}, C_{Yr}, $C_{Y\dot{\beta}}$.

Such requirements are included in the F-15 and B-1 contracts, for example. However the present requirements do not specify the method of determination of the derivatives, whether they should be obtained analytically or experimentally or, in the latter case, in what type of facility. This is left up to the contractor and, since the suitable experimental capabilities are scarce or, in most cases, non-existent, most derivatives are at the present time calculated by approximate methods. As discussed before, the accuracy of such predictions for conditions involving high angles of attack and high Reynolds numbers may sometimes be highly questionable.

More complete dynamic stability data than those presently available are also required in connection with certain new concepts and programs. Here belongs, for instance, the development of Control Configured Vehicles (CCV)

and various phases of the Advanced Development Program (ADP) on Stall/Spin such as the development of a stall inhibitor-departure preventor, and of automatic recovery controls. For CCV:s, in addition to the dynamic stability derivatives so far discussed, dynamic control derivatives such as control damping and higher frequency derivatives may also be of interest.

In addition to stability problems related to directly piloted military aircraft, dynamic stability considerations may also be of importance for current projects involving Remotely Piloted Vehicles (RPV), which because of their rather limited possibilities for onboard tuning of the stability augmentation devices may experience stability problems. The small inertia of these vehicles and the fact that some versions are designed for maneuvers at very high g:s, may render the aerodynamic coupling terms, such as represented by cross-derivatives C_{np} and $C_{\ell r}$, rather important. It should be remembered here that although RPV:s do not, of course, carry any pilots and are themselves rather inexpensive and therefore expendable, they may sometimes be used to carry extremely expensive equipment and may therefore be designed for recovery by another aircraft in which case the safety of that aircraft also becomes important. The dynamic stability of RPV:s

in free flight as well as in proximity to the mother aircraft should therefore be of some concern.

The flow around an aircraft or an RPV, and therefore its static and dynamic stability parameters, will of course be greatly affected by effects such as the interaction with engine inlet flow or the interaction due to the addition of stores. The engine inlet flow may be specially important for RPV:s, because of the large relative size of the engine as compared to the size of the entire vehicle. Any transient or oscillatory effects in the engine flow may also be of significance.

2.3 STOL Transport Aircraft

For STOL aircraft, such as the Advanced Medium Short Takeoff and Landing Transport (AMST) and the temporarily (?) postponed Quiet Experimental Short Takeoff and Landing Transport (QUESTOL) research aircraft, the dynamic stability information is of interest mainly for approach and landing conditions, where speeds as low as 75 kt. and 68 kt., respectively, and angles of attack of between 10° and 20° are envisaged. Several lift concepts are being considered for these aircraft, including the Externally Blown Jet Flap (EBF), the Internally Blown Jet Flap (IBF),

the augmentor wing, and the upper surface wing blowing. Rather complete sets of stability derivatives already exist for similar configurations with both a low (Ref. 20) and a high (Ref. 21) thrust-weight ratio; in both cases the effect of EBF or of a similar system was included and data were obtained for a sufficient range of angle of attack, flap settings and power settings, but at too low values of the Reynolds number. It is expected, however, that the Stability Augmentation System (SAS) can handle the possible differences in stability characteristics due to Reynolds number effects. More information may be needed for an analysis of flight characteristics, if SAS failed.

A sensitivity study presented in Ref. 22 indicates that the most important dynamic derivatives for a STOL transport aircraft are

C_{mq}, $C_{m\dot{\alpha}}$, $C_{\ell p}$, C_{nr} and C_{np}.

Since the angles of attack of interest are only moderately high, the power-off derivatives can be estimated with sufficient accuracy using standard prediction methods such as contained in the USAF Stability and Control DATCOM (Ref. 23), but taking into account the non-linearities with angle of attack. In most cases no satisfactory

methods to calculate the effects of the powered lift systems are available (Ref. 22). It is interesting to note that for the two different configurations and different powered lift systems investigated in Refs. 20 and 21, the application of power at higher angles of attack had almost completely opposite effects on the three damping derivatives: in Ref. 20 this effect was large on $C_{\ell p}$ but small on $(C_{mq} + C_{m\dot{\alpha}})$ and C_{nr}, whereas in Ref. 21 in most cases the effect was large on $(C_{mq} + C_{m\dot{\alpha}})$ but only moderate on C_{nr} and small or irregular on $C_{\ell p}$. In Ref. 20 the effects of both angle of attack and power on C_{np} were large and could be expected (Ref. 22) to have significant influence on flying qualities. In view of these non-uniform experimental results and the present inability to calculate the effects of power-on on the various derivatives, an experimental determination of all the dynamic derivatives mentioned in this section may be required for a STOL transport aircraft.

Since most of the dynamic stability information for this type of aircraft is needed for approach or landing conditions, it may be desirable to also investigate the effect on various derivatives of the moving ground. This effect can be simulated in several existing low-speed wind tunnels.

Another specific problem pertaining to STOL transport aircraft is the possible importance of the so-called "forward velocity derivatives". These derivatives, which usually can be obtained from other, already known, aerodynamic and thrust coefficients, are the result of a strong interaction that usually exists during low-speed, high-power flight between aerodynamics and thrust. They can affect the approach damping and frequency as well as the flight path stability.

2.4 Summary of Needs for Testing Capabilities

Summarizing the most important requirements for dynamic stability information for the categories of aerospace vehicles discussed in sections 2.1, 2.2 and 2.3, the following testing capabilities appear to be needed, in terms of the Mach number range, the angle-of-attack range, the type of dynamic derivative required and for as high a Reynolds number as can be provided in the presently existing or proposed wind tunnel facilities:

Speed Range	α	Derivatives required
subsonic (M<0.6)	$\alpha \leq 20^\circ$	C_{mq}, $C_{\ell p}$, C_{nr}, C_{np}, $C_{\ell r}$, $C_{m\dot{\alpha}}$, $C_{n\dot{\beta}}$
	$20^\circ \leq \alpha \leq 50^\circ$	C_{mq}, $C_{\ell p}$, C_{nr}, C_{np}, $C_{\ell r}$
	$40^\circ \leq \alpha \leq 90^\circ$	C_{mq}, $C_{\ell p}$, C_{nr}, C_{np}, $C_{\ell r}$; (incl. dependence on spin rate)
transonic (0.4≤M≤2)	$\alpha \leq 20^\circ$	C_{mq}, $C_{\ell p}$, C_{nr}, C_{np}, $C_{\ell r}$, $C^*_{m\dot{\alpha}}$, $C^*_{n\dot{\beta}}$, $C^*_{\ell\dot{\beta}}$
	$20^\circ \leq \alpha \leq 50^\circ$	C_{mq}, $C_{\ell p}$, C_{nr}, C_{np}, $C_{\ell r}$
supersonic (2≤M≤7)	$\alpha \leq 50^\circ$	C_{mq}, $C_{\ell p}$, C_{nr}, C^*_{np}, $C^*_{\ell r}$
hypersonic (M≥5)	$\alpha \leq 55^\circ$	C_{mq}, $C_{\ell p}$, C_{nr}

Of the derivatives listed, the three damping derivatives C_{mq}, $C_{\ell p}$ and C_{nr}, as well as the variation of the yawing moment with the rate of rotation in spin

$$C_n = f(rb/2V)$$

must in most cases be considered as being of the highest importance. The starred derivatives, on the other hand, seem to be of the lowest importance, and it appears probable that, after establishing their order of magnitude and their typical range of variations with α for one representative vehicle configuration, they need not be included in a complete dynamic stability testing program.

A simulation, as complete as possible, of flight Reynolds number constitutes, of course, one of the standard requirements for all kinds of aerodynamic testing*, and especially so at high angles of attack. Large efforts are presently being conducted to construct new facilities to satisfy this requirement as well as possible, despite various economical and technical constraints. It is not realistic to expect that any large facilities may be built specially for the purpose of dynamic testing. There is no need, therefore, to specify in this report any desirable values of Reynolds number other than by indicating that they should be as high as can be obtained at any particular time. It should be kept in mind, however, that after a certain amount of dynamic stability information, for several configurations and at various flow conditions, has been accumulated, it may be possible to review the situation again and perhaps to reduce the number of derivatives for which as complete as possible Reynolds number simulation is essential, thereby permitting some dynamic stability testing to be performed in smaller, less expensive, facilities.

3. EXPERIMENTAL CAPABILITIES AVAILABLE

Dynamic stability information can in principle be

---

* See, for example, Refs. 81 and 82.

obtained from model experiments in many different types of facilities. Here belong, for instance, tests in aero-ballistic or hypervelocity ranges, wind-tunnel tests with free-flying models, out-door free-flight tests using either rocket-propelled or radio-controlled gliding models, wind-tunnel free-flight tests using remotely controlled dynamic models, or spin-tunnel experiments. The latter three techniques are very well described in Reference 24. Together these three techniques cover the entire range of angles of attack of interest, from low angles up to and including the stall (wind-tunnel free-flight), through angles typical of post-stall and spin-entry motions (radio-controlled models) and to angles representative of developed spin and spin-recovery situations (spin-tunnel). All the techniques mentioned above, however, have one common disadvantage - they are not suitable for experiments at high Reynolds numbers. In addition, although some of them can be used for extraction of dynamic stability derivatives from the model motion history, this is rarely done. Thus the main use of these techniques is for visual studies of the stability characteristics and motions of the aircraft, all at low Reynolds numbers.

The only realistic possibility to obtain model-scale dynamic stability information at properly simulated

Reynolds and Mach numbers lies in performing captive-model experiments in high Reynolds number wind tunnels. The resulting static and dynamic stability derivatives and other aerodynamic data (such as the yawing moment as a function of the rate of rotation) can then be used in existing or improved (to include nonlinear formulations) methods of analysis to ultimately obtain a prediction of the stability characteristics and motions of the aircraft at high Reynolds numbers. This section, therefore, will be limited to a review of the available experimental capabilities for the measurement of dynamic stability derivatives using captive-model techniques in wind tunnels.

As mentioned before in this report, dynamic stability derivatives can also be extracted from full-scale flight tests. Since, however, the results of such tests are obtained too late to significantly affect the design of a new aircraft, the relevant techniques are not included here. Full-scale flight experiments are of course most essential for correlating the values of the various dynamic stability parameters and the flight behaviour of already existing aircraft. As discussed in the previous section, such correlations are badly needed for obtaining a better understanding of the relative importance of the various derivatives as well as for a realistic evaluation of the

presently used methods of analysis, especially with regard to the high angle-of-attack, stall and spin conditions.

The present survey is based on results of a questionnaire distributed to a certain number of organizations on the North American continent, as well as on discussions conducted during brief visits to various US government organizations such as:

NASA: Ames Research Center, Moffett Field, Cal.
Langley Research Center, Hampton, Va.
Low-Speed Aircraft Division
High-Speed Aircraft Division

USAF: Arnold Engineering Development Center, Tullahoma, Tenn.
von Karman Gas Dynamics Facility
Propulsion Wind Tunnel Facility

A list of persons interviewed during these visits is included in Appendix 1.

Although the survey covers only wind tunnel facilities in the USA and Canada, it should be kept in mind, that important capabilities for dynamic stability experiments exist also in some other countries of the world. The most significant of those can be found in the following organizations:

Office National d'Etudes et de Recherches Aerospatiales, France

Royal Aircraft Establishment, England

The Aeronautical Research Institute of Sweden

Royal Institute of Technology, Sweden
National Lucht - en Ruimtevaartlaboratorium,
The Netherlands.

This section contains a discussion of the questionnaire, a review of the wind tunnels equipped for measurement of dynamic stability derivatives, as well as a survey of capabilities for measuring different types of derivatives. This latter is divided according to the type of derivatives and includes pitch and yaw damping derivatives, rolling derivatives and all other derivatives, as separate sub-sections.

The survey is intended as a review of the presently available capabilities. Devices of the past, which no longer are operational, are not included. No details are given of the methods, techniques and equipment used, unless such details are essential to the proper understanding of the potential of the capability discussed and cannot easily be found elsewhere. Otherwise the reader is referred to the references given in the tables and to general papers on the subject of the measurement of dynamic stability derivatives, such as References 25 - 29, each of which also includes an excellent bibliography.

3.1 Questionnaire

In order to find out what wind tunnel capabilities exist in North America that could be used to meet the needs for dynamic stability information discussed in section 2, a brief survey of various government, commercial and university organizations was made. A suitable questionnaire was prepared (reproduced in Appendix 2) and distributed to 29 organizations, which, from the author's personal knowledge, were at least likely to have some capabilities in this field. Of the 25 returns received, 7 indicated no capabilities for dynamic stability testing at the present time, although one of them included the acquisition of such a capability in the long range plans for in-house activities. The results of the survey and the information contained in the present section are believed to constitute a representative description of the capabilities for measuring dynamic stability derivatives in the wind tunnels available in the United States and Canada. Altogether 18 organizations have capabilities in this field, although in some cases the status of these capabilities is not fully operational or their usefulness is severely restricted by the small size of the wind tunnel or by the rather simple nature of the apparatus. A list of organizations included in the survey is given in Appendix 3.

3.2 Wind Tunnels Included in the Survey

The 18 organizations in the USA and Canada that have capabilities for dynamic stability investigations together operate 39 wind tunnels that are suitably equipped for that kind of experiments. The main characteristics of these tunnels are listed in Tables 1-4, where for each tunnel the name and the type of the tunnel, the size of the test section, the Mach number range (or the wind speed range), the Reynolds number per foot, the total temperature, the dynamic pressure and the run time are given. Of the total number of wind tunnels listed, there are

12 Hypersonic (or Hypervelocity) Wind Tunnels (Table 1)

11 Supersonic Wind Tunnels (Table 2)

11 Transonic (including "Trisonic") Wind Tunnels (Table 3)

and 5 Subsonic Wind Tunnels (Table 4).

For 22 of these wind tunnels more details about their design and performance can be obtained from Ref. 30, and in these cases the corresponding page in that reference is also indicated in the tables. In cases where the information about the Mach number and the Reynolds number range of the wind tunnel were given differently in the questionnaire and in Ref. 30, the data of the questionnaire, being more

recent or perhaps more applicable to the performance of dynamic stability experiments, were used in Tables 1-4. For wind tunnels not included in Ref. 30, the tunnel data were compiled on the basis of other information available to the author. In a few cases where this information was not accessible, blank spaces had to be left in the tables.

It was not practical in this report to include the detailed information on the variation of Reynolds number with Mach number. This can be obtained, if necessary, from facility performance diagrams, which in many cases are given in Ref. 30. Such information can also in some cases be deduced in an approximate fashion, from the knowledge of the type of facility, which is given in the tables. Thus the numbers under the heading "Reynolds number per foot" indicate the range of Reynolds numbers for a range of Mach numbers, and for any particular conditions can only be considered as representative of the order of magnitude of the Reynolds number range applicable at that particular Mach number.

3.3 Facilities for Measuring Pitch and Yaw Damping

Existing facilities for the measurement of pitch and yaw damping derivatives are listed in Table 5. These two

damping derivatives are considered together, since in most cases the same apparatus can be used for both, by simply rotating the model by 90° around its longitudinal axis. For easier utilization, the table is sub-divided into sections, according to the Mach number range covered. Each entry consists of the name and the Mach number range of the wind tunnel, the typical length of an aircraft model, the range of Reynolds number based on model length, a few key words describing the method of measurement and the apparatus or model support, the range of angle of attack and the angle of sideslip at which the experiments can be performed, and references to papers describing the details of the apparatus and/or its application. There is also a column with "remarks" where any unusual features of the apparatus are noted or in which a reference may be made to an appendix, containing further details.

Unless otherwise specified it is assumed that the experimental procedure utilizes an oscillatory small-amplitude motion and that the maximum angles of attack and sideslip can be attained at the same time.

Several of the facilities listed in Table 5 may be used also for measuring derivatives other than pitch and yaw damping. If so, they will also be listed in some of

the subsequent tables. For instance, the two-degree-of-freedom apparatus at Calspan can also be used to determine derivatives due to vertical acceleration, the forced-oscillation rigs at NASA-LRC can also measure some cross-derivatives, etc. However, since the purpose of each table is to provide the reader with as complete information as possible about facilities that can be used for obtaining a particular derivative, all such facilities are included in each pertinent table.

Of those facilities which appear only in Table 5, the following additional details may be of interest:

In the 8-ft Transonic Wind Tunnel at Calspan the angles of attack or sideslip can be increased by means of special adapters. The model is pivoted on either a bearing or torsional spring mount through the center of gravity.

In the 20-inch Hypersonic Wind Tunnel at Fluidyne the model is attached, via an air bearing, to an aft-supported or a side-supported strut. A four-compartment or a two-compartment, respectively, phase blowing can be incorporated in the system.

In the 20-inch Supersonic Wind Tunnel and the 21-inch Hypersonic Wind Tunnel at JPL, a free-flight technique is

used, employing both the gun-launch or the wire-release technique. In the supersonic wind tunnel a spin head is incorporated in the gun-launch and the spin rate as well as the yaw/pitch amplitudes can be closely controlled. The initial angle of attack can be precisely set. Models can be delicately constructed to emphasize the data being obtained. Model wall temperature can be controlled down to T_w/T_∞ close to unity. The 6-degree-of-freedom unrestrained motion of the model is recorded on high speed movie film using camera speeds up to 500 frames a second. So far only bodies of revolution and various re-entry shapes have been investigated. The models are very small, and, therefore, the Reynolds numbers are very low. This technique is easily "portable" and can be used in many other wind tunnels by the JPL staff.

In the 4" x 4" Gasdynamic Wind Tunnel at the MIT Aerophysics Laboratory a free or a forced oscillation technique is employed using a magnetic balance. This technique is still under development. A similar technique is being developed for the 6 inch diameter Subsonic Wind Tunnel ($0<M\leq 0.4$) in the same laboratory (not included in the list of facilities because of its size and the developmental nature of the device).

In the 11-inch Helium Hypersonic Wind Tunnel and the 30-inch Trisonic Wind Tunnel at the NAE, pitch damping is measured employing the half-model technique. Supersonic experiments have been conducted (Ref. 2) with two models (of the space shuttle) oscillating at the same time, and in the presence of a simulated exhaust plume. Shadowgraph techniques have been developed using a high-speed movie camera and the half-model technique.

In the Supersonic Tunnel No 2 and the Hypersonic Tunnel No 8 at NOL, a 1 degree-of-freedom ball bearing pivot or a 3 degree-of-freedom spherical air bearing pivot are used to obtain large-amplitude ($\pm 15^{\circ}$) free-oscillation motions in either pitch or yaw around a zero mean angle of attack or sideslip. There is also a small-amplitude free-oscillation apparatus using a flexure pivot and a small-amplitude internally-driven forced-oscillation balance. Free-flight technique is also used, with a non-linear data-reduction capability. In the Hypervelocity Research Tunnel and the Hypervelocity Wind Tunnel at the same laboratory, there is a free-oscillation rig with a flexure pivot; in the Hypervelocity Research Tunnel this rig employs an electro-optical displacement follower for the remote sensing of model angular motion.

In the 3 transonic, 3 supersonic and 3 hypersonic wind tunnels at PWT and VKF, listed in Tables 1-3, there are 5 forced-oscillation and 8 free-oscillation balances for measurement of pitch or yaw damping. Of these, the forced-oscillation and the free-oscillation balances in the two 16-foot wind tunnels (16 T and 16 S) have a maximum normal force capability of 8000 lbs and 4500 lbs, respectively. A review of the existing dynamic stability balances at VKF and PWT is now in preparation (Ref. 59). Several new VKF and PWT balances, either recently completed or under construction, are described briefly in section 3.6.

It should be noted that Table 5 and the subsequent Tables 6 and 7 were prepared on the basis of the questionnaire and their accuracy depends on the accuracy of the material received. However, in a few instances, it was possible for the present author, from his own experience or knowledge, to correct certain errors, misrepresentations or omissions and to verify these corrections over the telephone. Otherwise the material is reproduced as received.

3.4 Facilities for Measuring Derivatives due to Rolling

The facilities for measuring derivatives due to rolling, that is derivatives $C_{\ell p}$, C_{np} and C_{Yp}, are listed in Table 6.

Methods of steady roll, roll decay, and forced- and free-oscillation in roll are included. The following additional material may be of interest:

The steady-state forced-roll apparatus*(rotary balance) which can be used in the 7 x 10 Foot High Speed Wind Tunnel at NASA-LRC-HS, is shown in Figure 2. The model is mounted on a six-component wire strain-gage balance of the type normally used for static tests of sting-supported models. The angle of attack can be varied by means of interchangeable couplings between the balance and the rotating sting support. The model is driven by a constant-displacement, reversible hydraulic motor located inside the main sting body. The speed of rotation is varied by controlling the fluid displacement in a hydraulic pump, which actuates the hydraulic motor. Corrections have to be applied to the data for deflection of the balance and support under load and for the centrifugal forces introduced by these deflections and by any initial displacement of the model CG from the roll axis.

The forced-oscillation roll mechanism which is compatible with either the 7 x 10-foot High Speed Wind Tunnel or the 8-foot Transonic Pressure Tunnel at NASA-LRC-HS, is shown in Figure 3. A 2-hp variable-speed motor is used to oscillate the sting and model by means of an offset crank. A torsion spring internal to the sting is connected

* Also used for tests at $\alpha = 90^{\circ}$, for studies of flat spin.

to the front of the strain-gage balance section and provides a restoring torque, which together with any aerodynamic spring balances out the model inertia, when the model is oscillated at velocity resonance. A system of resolvers, filters, and damped digital voltmeters is used to separate the torque signal into in-phase and out-of-phase components. The balance is designed for a maximum normal force of 1000 lbs. This principle of operation is similar to that used for the forced-oscillation pitch and yaw mechanism described in Ref. 50 and Ref. 65 and illustrated in Figure 4. Note however that the recent version of this apparatus employs a mechanical rather than hydraulic drive.

The new forced-oscillation roll mechanism for tunnels 4T, 16T, 16S, A, B and C at PWT and VKF, will be discussed in section 3.6.

So far in this section, and in Table 6, the derivatives due to rolling were denoted as derivatives due to the rolling velocity p. However, a rolling motion around a fixed body axis at an angle of attack causes also a simultaneous variation in the rate of change of the angle of sideslip, $\dot{\beta}$. Similarly, such a variation in $\dot{\beta}$ is also caused by a yawing motion in the body-axis system. Therefore, all the derivatives due to rolling and yawing in the body axis system, that are

obtained during experiments using fixed axes of oscillation or rotation (which applies to all the experimental methods so far discussed in sections 3.3 and 3.4) should, strictly speaking, be represented by expressions containing also the effects of $\dot{\beta}$. Also, and as already mentioned on p. 15, a pitching oscillation around a fixed axis results in combined effects due to both q and $\dot{\alpha}$. The complete expressions for the various rotary derivatives in a fixed body-axis system are, therefore:

$C_{\ell p} + C_{\ell\dot{\beta}} \sin\alpha$	$C_{nr} - C_{n\dot{\beta}} \cos\alpha$	$C_{mq} + C_{m\dot{\alpha}}$
$C_{np} + C_{n\dot{\beta}} \sin\alpha$	$C_{\ell r} - C_{\ell\dot{\beta}} \cos\alpha$	$C_{Nq} + C_{N\dot{\alpha}}$
$C_{Yp} + C_{Y\dot{\beta}} \sin\alpha$	$C_{Yr} - C_{Y\dot{\beta}} \cos\alpha$	$C_{Aq} + C_{A\dot{\alpha}}$

Since $\dot{\alpha}$ and $\dot{\beta}$ derivatives are only very rarely separated experimentally (see sections 3.5 and 3.6) and since some of them (but not all, see section 2) represent second order effects, the abbreviated rather than the complete notation has mostly been used throughout this report (as already indicated on page 17), to simplify the presentation. However, when discussing the separate effects of q and $\dot{\alpha}$ or of r and $\dot{\beta}$ (as will be done in the next two sections), the use of the complete expressions may occasionally be required.

In the list of available equipment that can be employed for measuring the dynamic derivatives due to rolling, there is an occasional mention of Magnus balances. It is recognized that more balances of that type may exist on the North American continent, in establishments which are concerned primarily with ordnance. Since, however, the subject matter of the present report was dynamic stability testing of aircraft, no effort has been made to make the list of Magnus balances complete.

3.5 Facilities for Measuring Other Dynamic Derivatives

It remains to review facilities where the dynamic cross-derivatives other than those due to rolling, and the derivatives due to linear acceleration (i.e. due to $\dot{\alpha}$ or $\dot{\beta}$ motions) can be measured. These facilities are summarized in Table 7. The following additional comments may be of interest.

In the 8-Foot Transonic Wind Tunnel at Calspan (CAL), a 2-degrees-of-freedom (2 DOF) mechanically driven forced-oscillation apparatus can be used to separate the derivatives due to q and $\dot{\alpha}$ effects (or, alternatively, by rotating the model, r and $\dot{\beta}$-effects). A pure pitching (q) motion or a pure plunging ($\dot{\alpha}$) motion can be simulated, as well as any

combination of the two. The frequency range is from 3 to 12 cps and the amplitudes of up to $\pm 5^{\circ}$ or ± 0.5 ft and accelerations of up to 200 rad/sec^2 or 20 g:s can be employed in the rotational or translational case, respectively. The normal force capability, at the model center of gravity, is 1200 lbs. The apparatus has not been used for some time and the electronics part of it, including the instrumentation used for data analysis, may need updating. Models could be installed at angles of attack up to 10° or 20°, using bent stings, subject to load limitations.

Similar concepts were employed in the past at NASA-LRC to obtain pure yawing (r) and acceleration-in-sideslip ($\dot{\beta}$) effects (Refs. 66, 67). It is not known to the author, whether these capabilities still exist. The only other existing method to separate the q and $\dot{\alpha}$ (or r and $\dot{\beta}$) effects is by experiments conducted in a test section with curved flow (see e.g. Refs. 67-69). Such a test section was once installed in the NASA-LRC (low speed) Stability Tunnel which is now available at the Virginia Polytechnic Institute. An apparatus, under construction at NAE, for separation of the q and $\dot{\alpha}$ effects, will be mentioned in the next section.

In the Full-Scale Tunnel at NASA-LRC the forced-oscillation apparatus is capable of measuring all the dynamic moment and force derivatives due to rolling, yawing

and pitching around a fixed axis, for angles of attack or sideslip of up to 90°. The amplitude range is variable and can be as high as $\pm 30^{\circ}$. Experiments can be performed also with powered models. A 6-component interaction-free balance is used with on-line data reduction. A sketch of the apparatus set up for yawing oscillation is shown in Fig. 5. The oscillatory motion is imparted to the model by means of a flywheel-driven system of pushrods and bell-cranks powered by a 3 h.p. electric motor. The frequency of oscillation (typically 0.5 - 1.5 cps) is varied by changing the speed of the motor. Voltage signals proportional to the sine and cosine of the flywheel rotation angle are generated by a precision sine-cosine potentiometer.

The forced-oscillation apparatus used in the 7x10 Foot High Speed Tunnel, the 8-Foot Transonic Pressure Tunnel and the Unitary Plan Wind Tunnels at NASA-LRC has recently been modified, adding the capability to measure the derivative C_{ℓ_r}. No pertinent information has yet been published but the initial results are considered promising.

3.6 New Facilities for Measuring Dynamic Derivatives

In an early recognition of the present revival of interest in the dynamic stability characteristics of aircraft, several organizations have already embarked,

in the last year or so, on the design and construction of new, more advanced, pieces of apparatus. Some of these are already completed and are being calibrated. Some are only at the proposal stage. In this section some of the more important recent developments will be briefly summarized.

A continuous rotation (rotary balance) apparatus (Fig.6) was installed in the Full Scale Tunnel at NASA-LRC in February 1973. This apparatus is included in Tables 5-7. It makes use of a 6-component balance and high-speed magnetic-tape data acquisition. It is capable of a maximum rate of rotation of 200 rpm (resulting in a maximum value of the dimensionless spin rotation parameter, $\Omega b/2V$, of 0.4) and will allow a spin radius of up to 1 foot for a model weight of 80 lbs. This means that it will be possible to employ the same models as those presently used for the outdoor radio-controlled model experiments (drop-test models). The construction of such models has recently been greatly simplified (utilizing hobby-type radio-controls, etc.) and as a result the cost of a model of a modern fighter aircraft is down to $30,000 or so. By slightly tilting the principal axis of rotation of the apparatus (such a capability not included at the present time), the determination of a number of dynamic derivatives as functions of the spin rate may become possible (details on the accuracy of such a technique not yet available, see p. 59).

Since the forced-oscillation roll apparatus described in section 3.4 (Ref. 64) is too large to allow its use in the Unitary Plan Wind Tunnel (4' x 4') at NASA-LRC, a special adapter has been constructed to replace the top part of the present forced-oscillation pitch-and-yaw apparatus (Refs. 70-73), which is used in that tunnel as well as in the 7 x 10-Foot High Speed Tunnel and the 8-Foot Transonic Pressure Tunnel. This adapter will permit obtaining derivatives $C_{\ell p}$ and C_{np} in all these tunnels. It will accept normal forces up to 1000 lbs. (For static load limits on all the dynamic balances at NASA-LRC-HS, see Appendix 7.).At the present time this new adapter is being tested and it is expected that it may become operational by July 1973. This apparatus like many other oscillatory balances, requires special models (often made of aluminum, magnesium and fiber glass) of moderate inertia and with an inside cylindrical space of a larger diameter than for use with the conventional static-force balances. This differs from the requirements of e.g. the steady-state forced-roll apparatus in the 7 x 10 Foot High Speed Tunnel, for which conventional force-tests models are often acceptable.

In the 6 x 6-Foot Supersonic Tunnel at NASA-ARC experiments are now being conducted with a coning- and spinning-motion apparatus (Ref. 74), in many aspects similar

to the previously described steady-state forced-roll apparatus at NASA-LRC-HS. This new apparatus is capable of coning rates up to 600 rpm, obtained by means of a hydraulic drive motor. An electric spin motor located in front of the six-component balance inside the model can rotate the model around its longitudinal axis through a range of speeds up to 600 rpm (of interest only to Magnus measurements). The angle of attack can be fixed at various values between 0° and 30° by means of interchangeable bent stings. Within its range of angle of attack the apparatus satisfies some of the requirements put forward in Ref. 6, where it was shown that a nonlinear moment system for an arbitrary motion of an aircraft-like configuration (i.e. without the necessity of restricting the analysis to bodies of revolution) can be considered as being composed of moment contributions resulting from four characteristic motions (in the body-axis system), namely (a) steady flight, (b) coning motion, (c) yawing, and (d) pitching - all at an angle of attack. Of these four motions the coning apparatus is capable of reproducing the first two. Experiments are still* being conducted to investigate whether by tilting the axis of rotation of the apparatus by a few degrees, the derivatives due to yawing and pitching can also be obtained with sufficient accuracy.

---

* as of March 3, 1973.

A forced-oscillation, basically one-degree-of-freedom apparatus (Ref. 75) was employed for a number of years in the three sections of the Unitary Plan Wind Tunnel at NASA-ARC. The various components of pitch, yaw and roll were all obtained by varying the axis of oscillation. The forcing system comprised a feedback loop in which velocity feedback was used to excite and control the amplitude of the model oscillation. The data reduction was greatly simplified by limiting the angular displacements around the two axes perpendicular to the axis of oscillation to very small values and at the same time by making the mechanical stiffnesses around those two axes very large. The apparatus was capable of measuring all the three damping derivatives C_{mq}, $C_{\ell p}$, C_{nr} as well as the cross derivatives C_{np} and $C_{\ell r}$. To obtain a complete set of derivatives 3 experiments were required, using two interchangeable balances, $2\frac{1}{2}$" diameter, one for oscillation in roll and one for pitch (yaw). Special light models were required, and the models had to be trimmed and balanced (as in many other oscillatory experiments). The apparatus could accept normal forces of the order of 500 lbs. Frequencies of the order of 4-12 cps were employed. The apparatus was successfully used for several investigations, such as described in Refs. 76-80. Although not operational at the present time, it could probably be restored or even reconstructed in a scaled-up version, and with a thoroughly updated electronic control system. This is the reason for

including it in the present section.

A forced-oscillation pitch or yaw apparatus is presently being put into operation* in the 30-inch Wind Tunnel at NAE. A preliminary sketch of the apparatus is shown in Fig. 7. The elastic constraints are provided by an orthogonal system of three mutually intersecting cruciform elements and the excitation is provided by means of an electromagnetic exciter. All reactions are resolved into in-phase and out-of-phase components and the signal-to-noise ratio is maintained at a high level through the use of a lock-in amplifier system. Semiconductor gages are used throughout. Preliminary results appear very promising. Prospects for scaling-up the apparatus for use in larger wind tunnels are good; however, for such a larger version, which implies lower frequencies, another form of excitation may be preferable. There is also a good possibility to modify the present design in such a way as to incorporate, in the same balance, an alternative capability of forcing the oscillation in roll. If this can be achieved, a complete set of dynamic derivatives about a fixed axis could be obtained. This apparatus is included in Tables 5 and 7.

A forced-oscillation apparatus for plunging motion is being constructed for the 30-inch Wind Tunnel at NAE, taking

---

* This development is partly supported by a NASA contract.

advantage of the already existing equipment for dynamic stability testing using half models. Instrumentation similar to that described above will be used. The apparatus will be capable of measuring the vertical acceleration derivative, $C_{m\dot{\alpha}}$.

A forced-oscillation pitch or yaw apparatus (Fig. 8) has recently been put into operation at VKF and PWT, to be used in the 3 ft, 4 ft and 16 ft supersonic and hypersonic wind tunnels at the two facilities. The apparatus utilizes a cross-flexure pivot, a one-component moment balance and an electric shaker motor. Another mechanism, a forced-oscillation roll apparatus (Fig. 9), has also recently been completed. It utilizes a water-jacketed, five-component balance, twin beam flexures, roller bearings to support the loads and electric printed-circuit drive motors. In both mechanisms the flexures are instrumented to measure the pertinent displacement and also provide a restoring moment which cancels the inertia moment when the system is operating at its natural frequency. Both mechanisms can support models with a combined loading of 1200 lb normal force and 300-lb axial force at angles of attack up to 28°. Precise frequency measuring and phase resolving instrumentation is used, together with a tunnel scanner and a computer, to obtain the dynamic derivatives $C_{\ell p}$, C_{np}, C_{Yp}, C_{mq} and C_{nr} (but not $C_{\ell r}$). Experiments have already been conducted

with the AGARD Models B and C in Tunnel A at VKF and with a 0.024 scale model of B-1 at $\alpha < 10^{\circ}$ in Tunnel 16 S at PWT. In general good accuracy has been experienced, except for cross-derivatives for models with high values of the product of inertia I_{xz}. The results have also been found to be very sensitive to flow disturbances (which, of course, is not at all unusual for this type of experiment).

A forced-oscillation pitch apparatus (Fig.10) is presently being calibrated in Tunnel 4 T at PWT. This apparatus is mainly intended for blunt configurations at high angles of attack. A cross-flexure pivot is used and the frequency is adjusted by interchanging a cantilever spring. The damping torque and the amplitude are the quantities measured. The apparatus can also be used in a free-oscillation mode using air-jet excitation. Normal force up to 600 lbs can be accepted. This apparatus eventually may be scaled up for use in Tunnels 16 S and 16 T.

Finally, a forced-oscillation roll apparatus (Fig. 11) is being designed for Tunnels 16 S and 16 T at PWT. The principle of the design and operation appears to be similar to the one just described. This apparatus is being designed for normal forces up to 4000 lbs, amplitudes of $\pm 2^{\circ}$ and frequencies in the range 1-15 cps. High angle-of-attack (up to 45°) application is envisaged. The completion is scheduled for late 1973 or early 1974.

4. NEEDS VERSUS EXISTING CAPABILITIES

The needs for dynamic stability information, as discussed in section 2 are compared in Table 8 with the existing capabilities for obtaining this information, as discussed in section 3. The left-hand side of the table is reproduced from section 2.4 and the right-hand side represents a synthesis of the information contained in section 3 and Tables 5-7. The organizations given on the right-hand side of the table are those which have the capabilities listed on a given line and at the same time can provide as high a Reynolds number as possible. A bracket indicates that this particular item is not compatible with all the other, unbracketed, items on the same line. A square bracket around a derivative indicates that this particular capability is still under development or has not yet become fully operational.

By comparing the left-hand side of the table with the right-hand side, all the discrepancies between what is needed and what is now available are immediately revealed. Apart from smaller differences in ranges of Mach number and angle of attack covered, the single most important discrepancy between what is needed and what is now available is:

For Mach numbers higher than 0.1, no wind-tunnel capabilities exist at the present time for measuring <u>any</u> dynamic derivatives of aircraft at angles of attack higher than 25° .

(with the exception of $C_{\ell p}$ at $M < 0.4$, and C_{mq} and C_{nr} at $M = 12$ and 14 at $\alpha = 30°$)

An additional and very important discrepancy which is not evident from Table 8, but which is known from general experience with simulation capabilities of the existing wind tunnels is:

No wind-tunnel capabilities exist at the present time for measuring dynamic derivatives of aircraft at fully simulated flight Reynolds numbers.

On the other hand, Table 8 indicates that significant wind-tunnel capabilities now exist to measure most of those dynamic derivatives that have been defined as important (in their various speed ranges) in this report, but always at low angles of attack (usually not exceeding 15° - 25°) and always at a Reynolds number that is significantly lower than the flight Reynolds number. At

low angles of attack, however, the deficiency in Reynolds number may not be as serious, or alternatively may be corrected by some of the methods indicated in section 2.

5. SUMMARY AND RECOMMENDATIONS

A review has been performed of the future needs for dynamic stability information for such vehicles as the space shuttle, STOL transport and advanced high-performance military aircraft, all of which are characterized by flying, at least during some portions of their trajectory, at much higher angles of attack than those which were typical of aircraft of the past. It was found that under those flight conditions, dynamic stability derivatives may undergo variations so large that they are much more likely than in the past to significantly affect the flight behaviour of aircraft. Although it appears that no realistic sensitivity studies have so far been performed for such flight conditions, it was possible to determine, in a tentative fashion, what dynamic derivatives may be of importance in the various ranges of speed and angle of attack. This assessment was based on an extrapolation of certain results on the high-speed steady flows around modern aircraft configurations as well as of information on the low-speed dynamic derivatives that have been measured for such configurations. Although this approach was often

based on conjectures rather than hard facts, it represents the best that could be done under present circumstances. That the problem is real enough and that our understanding of dynamics of flight at high angles of attack is not satisfactory at the present time and should be greatly improved, is best witnessed by the large number of out-of-control accidents which happen every year. It was suggested in this report that although our mathematical methods of analysis certainly are not adequate for such flight conditions and could be improved or replaced by other - more sophisticated - methods, the most efficient attempt to remedy the present situation seems to be to improve our knowledge of the aerodynamics (including dynamic derivatives), of the high angle-of-attack flight. The importance of the proper simulation of Reynolds number at these flight conditions was also pointed out.

A survey was then conducted of the existing capabilities, on the North American continent, to measure dynamic derivatives of aircraft at high angles of attack and at as-high-as-possible Reynolds number. A list of wind tunnels, in all speed ranges, that are equipped for this type of measurements, was compiled, and the experimental capabilities for measuring the various categories of dynamic derivatives in various ranges of speeds and angles of attack were reviewed. The more interesting or more advanced pieces of experimental equipment were then discussed in some detail.

After comparing the needs with the existing capabilities, two principal conclusions were reached:

(a) that, for Mach numbers higher than 0.1, no wind-tunnel capabilities now exist for measuring any dynamic derivatives of aircraft at angles of attack higher than 25° (with two minor exceptions), and

(b) that no wind-tunnel capabilities at all now exist for measuring dynamic derivatives of aircraft at fully simulated flight Reynolds numbers.

It is therefore recommended that experimental equipment be constructed, which would be compatible with large, high-pressure wind tunnels in all speed ranges, but especially up to Mach number 1.5, and which would be capable of measuring all three damping derivatives and in addition, for speed ranges listed in Table 8, also certain specified cross-derivatives and derivatives due to linear acceleration. It is essential that these measurements be made at angles of attack up to 50° (or even 55°) for all speed ranges and up to 90° for Mach numbers less than 0.6. For angles of attack between 40° and 90° at Mach numbers up to 0.6 equipment is also needed for determining the variation of various aerodynamic reactions, including dynamic derivatives, with the rate of rotation

in a spin. In addition, although this point has not been mentioned before in this report, the equipment for higher angles of attack should be capable of measuring dynamic cross-coupling derivatives, that is derivatives of longitudinal moments due to lateral motions, such as C_{mr} and C_{mp}, and vice-versa, such as C_{nq} and $C_{\ell q}$. In the presence of asymmetric flow conditions, typical of flight at a high angle of attack, and in the presence of spin rotation, these derivatives can no longer be considered negligible and may, in fact, play an important role during spin entry or spin recovery.

It should be noted that even in situations when the variation with the rate of rotation in a spin is of no interest, such as the case may be at lower angles of attack, the combination of the oscillatory motions in yaw and in pitch with the coning motion can still give, according to Ref. 6, a complete set of dynamic information (without the need for performing separate rolling oscillations) provided that for each motion the in-phase and out-of-phase components of all three moments are obtained (see p. 59). As explained in Ref. 6, such information can then be transposed, if desired, into the conventional stability derivatives, as used in the present report. It should also be mentioned, that the theory of Ref. 6, which is equivalent to a linearization around arbitrary values of α and β, but which so far was

linearized only around the zero rate of coning, is now being extended to include linearization around an arbitrary (constant) coning rate as well.

Depending on the results of the exploratory experiments which are now being conducted at NASA-ARC with the coning-motion apparatus (p. 58), several possible options for the conceptual design of the necessary equipment can be envisaged. If a complete set of dynamic moment derivatives can be obtained with such an apparatus with a sufficient accuracy, then a scaled-up rotary balance of this type (or of a type just installed in the NASA-LRC Full Scale Tunnel, p. 57) with the capability of setting angles of attack up to 90° and of tilting the axis of rotation a few degrees, would be able to measure the required dynamic derivatives as functions of both the angle of attack and the rate of rotation. Another possible arrangement would be the installation of a forced-oscillation pitch-and-yaw apparatus between the model and an untilted rotary balance, thereby obtaining the required combination of the oscillatory and coning motions. In such a case, however, the forced-oscillation apparatus must have the capability of measuring the in-phase and out-of-phase components of all three moments. Of all the forced-oscillation balances described in this report, only the apparatus now under development at NAE (p. 61) is designed to have such a capability; however it is not known yet how successful this apparatus turns out to be, and whether it will be possible to scale

it up to meet the full-scale load requirements, especially for a combination of high angle-of-attack and high rate-of-coning conditions.

If, for technical or economical reasons, the construction of the necessary equipment, as outlined above, is delayed, a rather incomplete set of derivatives in the range of angle of attack up to 50^{o} (and without simulating the coning motion) could be obtained, as an interim measure, using a conceptual design based on one of the following apparatuses, all of them still under development or being tested: (1) a combination of the forced-oscillation pitch-and-yaw apparatus (p. 52 and 56) and the forced-oscillation roll apparatus (p. 51 and p. 58) at NASA-LRC, with the indicated modifications and extensions, (2) a combination of the forced-oscillation pitch-and-yaw apparatus and the forced-oscillation roll apparatus at VKF (p. 62), which, however does not have the capability of measuring C_{ℓ_r}, (3) the forced-oscillation pitch-and-yaw apparatus, with an added capability for oscillation in roll, at NAE(p. 61) and finally, (4) a scaled-up and updated version of the old forced-oscillation, one-degree-of-freedom apparatus (p. 61), consisting of two balances, which was used at NASA-ARC in the past. The final choice between these options would have to await the outcome of the experiments which are now being conducted.

If, after obtaining the first sets of static and dynamic stability data at high angles of attack and high Reynolds numbers, the stall and spin characteristics of an aircraft can be predicted successfully, then it is recommended that the dynamic stability testing be in the future scheduled early enough to be able, if necessary, to significantly influence the design of the aircraft. The effect of varying the aircraft configuration, such as by design changes, the addition of stores, etc., on the dynamic stability derivatives, should also be considered while still in the planning stage, so that their influence on the flight behaviour and on the handling qualities of the aircraft can be predicted as early as possible.

6. ACKNOWLEDGMENT

The author is indebted to Vic Peterson and Gerry Malcolm of Ames Research Center who initially set up and monitored respectively, this project, and to all the persons listed in Appendices 1 and 3 for the most useful discussions during the author's visits to their organizations and/or for their assistance in obtaining the material necessary for this survey.

REFERENCES

1. Reding, J. P.
   Ericsson, L. E.
   Delta wing separation can dominate shuttle dynamics
   AIAA Paper 72-976, 1972

2. Orlik-Rückemann, K.J.
   LaBerge, J. G.
   Hanff, E. S.
   Supersonic dynamic stability experiments on the space shuttle
   AIAA Paper 72-135, 1972

3. Orlik-Rückemann, K. J.
   Iyengar, S.
   Effect of dynamic interference on the shuttle abort separation maneuver
   NRC NAE HSAL-M-151, 1972

4. Uselton, R.
   Wallace, A. R.
   Dynamic stability testing of space shuttle configurations during abort separation at Mach numbers 1.76 and 2
   AEDC-TR-71-198, 1971

5. Tobak, M.
   On the use of the indicial function concept in the analysis of unsteady motions of wings and wing-tail combinations
   NACA Report 1188, 1954

6. Tobak, M.
   Schiff, L. B.
   A nonlinear aerodynamic moment formulation and its implications for dynamic stability testing
   AIAA Paper 71-275, 1971

7. Wykes, J. H.
   Casteel, G. R.
   Collins, R. A.
   An analytical study of the dynamics of spinning aircraft. Part 1: Flight test data analyses and spin calculations
   WADC TR 58-381, 1958

8. Neihouse, A. I.
   Klinar, W. J.
   Scher, S. H.
   Status of spin research for recent airplane designs
   NASA TR R-57, 1960 (1957)

9. Chambers, J. R.
   Anglin, E. L.
   Bowman, J. S. Jr.
   Effects of a pointed nose on spin characteristics of a fighter airplane model including correlation with theoretical calculations
   NASA TN D-5921, 1970

10. Anglin, E. L.
Grafton, S. B.
Results of static and dynamic force tests of a 1/11-scale model of the F-4 airplane and their applicability to theoretical spin analysis
NASA TM SX-2124, 1970

11. Grafton, S. B.
Libbey, C. E.
Dynamic stability derivatives of a twin-jet fighter model for angles of attack from -10° to 110°
NASA TN D-6091, 1971

12. Grafton, S. B.
Anglin, E. L.
Dynamic stability derivatives at angles of attack from -5° to 90° for a variable-sweep fighter configuration with twin vertical tails
NASA TN D-6909, 1972

13. Steinmetz, G. G.
Parrish, R. V.
Bowles, R. L.
Longitudinal stability and control derivatives of a jet fighter airplane extracted from flight test data by utilizing maximum likelihood estimation
NASA TN D-6532, 1972

14. Parrish, R. V.
Steinmetz, G. G.
Lateral stability and control derivatives of a jet fighter airplane extracted from flight test data by utilizing maximum likelihood estimation
NASA TN D-6905, 1972

15. Bihrle, W. Jr.
Heyman, A. C.
The spin behaviour of aircraft
Grumman Aircraft Engineering Corp
GAEC Rept 394-68-1, 1967

16. Bihrle, W. Jr.
Influence of the static and dynamic aerodynamic characteristics on the spinning motion of aircraft
Journal of Aircraft, vol. 8, no. 10, pp. 764-768, 1971

17. Chalk, C. R.
Neal, T. P.
Harris, T. M.
Pritchard, F. E.
Woodcock, R. J.
Background information and user guide for MIL-F-8785B(ASG), "Military specification - flying qualities of piloted airplanes"
AFFDL-TR-69-72, 1969

18. Hall, G. W., Boothe, E. M. — An in-flight investigation of lateral-directional dynamics for the landing approach AFFDL-TR-70-145, 1970

19. Boothe, E. M. Parrag, M. L. — Evaluation of lateral-directional handling qualities and roll-sideslip coupling of fighter class airplanes AFFDL-TR-72-36 (vol. 1), 1972

20. Freeman, D. C. Jr Grafton, S. B. d'Amato, R. — Static and dynamic stability derivatives of a model of a jet transport equipped with external-flow jet-augmented flaps NASA TN D-5408, 1969

21. Grafton, S. B. Parlett, L. P. Smith, C. C. Jr. — Dynamic stability derivatives of a jet transport configuration with high thrust-weight ratio and an externally blown jet flap NASA TN D-6440, 1971

22. Laudeman, E. C. — STOL transport stability and control derivative prediction methods and accuracy requirements AIAA Paper 72-780, 1972

23. Ellison, D. E. Hoak, D. E. — USAF Stability and Control Datcom WADD TR-60-261 (continuously revised)

24. Chambers, J. R. — Status of model testing techniques, In the Proceedings of the AFFDL/ASD Symposium on Stall/Post-Stall/Spin, December 1971

25. Arnold, L. — Dynamic measurements in wind tunnels AGARDograph 11, 1955

26. Orlik-Rückemann, K. J. — Methods of measurement of aircraft dynamic stability derivatives NRC, Canada, LR-254, 1959

27. Bratt, J. B. — Wind-tunnel techniques for the measurement of oscillatory derivatives ARC R&M 3319, 1960

28. Dayman, B. Jr. — Free-flight testing in high-speed wind tunnels AGARDograph 113, 1966

29. Schueler, C. J.
Ward, L. K.
Hodapp, A. E. Jr.
Techniques for measurement of dynamic stability derivatives in ground testing facilities
AGARDograph 121, 1967

30. Pirrello, C. J.
Hardin, R. D.
Heckart, M. V.
Brown, K. R.
An inventory of aeronautical ground research facilities. Volume 1 - Wind Tunnels
NASA CR-1874, 1971

31. Walchner, O.
Sawyer, F. M.
Koob, S. J.
Dynamic stability testing in a Mach 14 blow-down wind tunnel
J. of Spacecraft and Rockets, Vol. 1, No. 4, pp. 437-439, 1964

32. Ibrahim, S. K.
Pollock, R. B.
Smith, K. W.
Christopherson, C. D.
Wind tunnel tests employing temporal and spatial variations in mass transfer distribution through a conical surface to control aerodynamic pitching moment characteristics
Fluidyne Eng. Corp. Rep. 0414-3-31-67, 1967

33. Grimes, J. H. Jr.
Casey, J. J.
Influence of ablation on the dynamics of slender re-entry configurations
Journal of Spacecraft and Rockets, Vol. 2, No. 1, pp. 106-108, 1965

34. Orlik-Rückemann, K. J.
LaBerge, J. G.
Adams, P. A.
Conlin, L. T.
A wind tunnel apparatus for dynamic stability experiments on sting-mounted slender bodies
NRC, Canada, NAE LTR-UA-13, 1970

35. Jaffe, P.
Obtaining free-flight dynamic damping of an axial symmetric body (at all angles of attack in a conventional wind tunnel)
JPL TR 32-544, 1964

36. Prislin, R. H.
High-amplitude dynamic stability characteristics of blunt 10-degree cones
JPL TR 32-1012, 1966

37. Prislin, R. H.
Wilson, M. B.
Determination of aerodynamic damping coefficients from wind-tunnel free-flight trajectories of non-axisymmetric bodies
JPL TR 32-1159, 1967

38. Dayman, B. Jr.
Comparisons between sting-supported and free-flight tests in the JPL Hypersonic Wind Tunnel on a modified Saturn-Apollo launch configuration (contains information on control of model wall temperature down to T_w/T_∞ = unity)
AIAA Paper 71-265, 1971

39. Jaffe, P.
Non-planar tests using the wind-tunnel free-flight technique (contains information on spinning models-launching and data reduction)
AIAA Paper 72-983, 1972

40. Regan, F. J.
Horanoff, E. V.
Hypersonic pitch damping support using water-cooled ball bearings
U.S. Naval Ordnance Lab, White Oak, Maryland, NOLTR 68-4, 1968

41. Darling, J. A.
Static-stability and roll-damping coefficients for a slender blunted cone showing the effects of spin, angle of attack, and center-of-gravity offset at Mach 5 and 7.7
U.S. Naval Ordnance Lab, White Oak, Maryland, NOLTR 69-232, 1969

42. Regan, F. J.
Iandolo, J. A.
Instrumentation, techniques and analysis used at the Naval Ordnance Laboratory for the determination of dynamic derivatives in the wind tunnel
U.S. Naval Ordnance Laboratory, White Oak, Maryland, NOLTR 66-23, 1966

43. Glowacki, W. J. et al.
The NOL Hypervelocity Wind Tunnel
AIAA Paper 71-253, 1971

44. Millard, W. A.
Curry, W. H.
A thin strap support for the measurement of the dynamic stability characteristics of high-fineness-ratio, wind-tunnel models
J. of Spacecraft and Rockets, Vol. 7, No. 7, pp. 854-858, 1970

45. Moore, D. R.
Stalmach, C. J.
Pope, T. C.
Investigations of ablation effects on hypersonic dynamic stability of a 10° cone
AFFDC-TR-66-230, 1967

46. Stalmach, C. J.
Lindsey, J. L.
Pope, T. C.
Investigation of oscillatory mass-addition effects on stability of a 10° cone at Mach 17
AFFDL-TR-69-127, 1970

47. Moore, D. R.
Stalmach, C. J.
Pope, T. C.
Jenkins, J. E.
Dynamic stability wind tunnel tests of a 10° cone with simulated ablation at M = 17
AIAA Paper No. 66-757, AIAA Aerodynamic testing conference, Los Angeles, California, Sept. 1966 (also published in AIAA Journal, Vol. 8, No. 6, June 1970)

48. Stalmach, C. J.
Lindsey, J. L.
Pope, T. C.
Hypersonic aerodynamic measurements on a 10° cone with oscillatory mass addition
AIAA 8th Aerospace Sciences Meeting, New York, January 1970, Paper No. 70-217

49. Maloy, H. E. Jr.
A method for measuring damping-in-pitch of models in supersonic flow
BRL Report 1078, 1959

50. Bielat, R. P.
Wiley, H. G.
Dynamic longitudinal and directional stability derivatives for a 45° sweptback-wing airplane model at transonic speeds
NASA TM X-39, 1959

51. Wright, B. R.
Kilgore, R. A.
Aerodynamic damping and oscillatory stability in pitch and yaw of Gemini configurations at Mach numbers from 0.50 to 4.63
NASA TN D-3334, 1966

52. O'Neill, E. B.
Phillips, K. A.
A description of 4 wind tunnel dynamic measuring techniques
DTMB Report 2296, 1967

53. Statler, I. C.
Tufts, O. B.
Hirtreiter, W. J.
The development and evaluation of the CAL/AF dynamic wind-tunnel testing system
AFFDL-TR-66-153, 1967
(also CAL TB-1555-S-1)

54. Orlik-Rückemann, K. J.
Iyengar, S.
LaBerge, J. G.
Comparison of three oscillatory techniques for cones at incidence
AIAA Paper 72-1015, 1972

55. Orlik-Rückemann, K. J.
LaBerge, J. G.
Static and dynamic longitudinal stability characteristics of a series of delta and sweptback wings at supersonic speeds
NRC, Canada, LR-396, 1966

56. Mockapetris, L. J.
A forced oscillation system for measuring damping derivatives at subsonic and transonic speeds
NSRDC Report 2627, 1967

57. Chambers, J. R.
Grafton, S. B.
Static and dynamic longitudinal stability derivatives of a powered 0.18 scale model of a fan-in-wing VTOL aircraft
NASA TN D-4322, 1968

58. Chambers, J. R.
Grafton, S. B.
Investigation of lateral-directional dynamic stability of a tilt-wing V/STOL transport
NASA TN D-5637, 1970

59. Uselton, J. C. (Ed.)
Dynamic Stability Measurement Capabilities in the AEDC wind tunnels
(in preparation)

60. Walchner, O.
Sawyer, F. M.
Durham, T. A.
Hypersonic wind tunnel measurements of roll damping derivatives for cones
ARL 69-1070, 1969

61. Regan, F. J.
Schermerhorn, V. L.
Supersonic Magnus measurements of the ten-caliber army-navy spinner projectile with wrap-around fins
NOLTR 70-211, 1970

62. Henderson, W. P.
Phillips, W. P.
Gainer, T. G.
Rolling stability derivatives of a variable-sweep tactical fighter model at subsonic and transonic speeds
NASA TN D-3845, 1967

63. Hayes, W. C. Jr.
Kemp, W. B. Jr.
Thompson, W. E.
Wind tunnel measurements and estimated values of the rolling stability derivatives of a variable-sweep airplane configuration at subsonic and transonic speeds
NASA TM X-600, 1961

64. Boyden, R. P.
Effects of leading-edge vortex flow on the roll damping of slender wings
Journal of Aircraft, Vol. 8, No. 7, 1971

65. Braslow, A. L.
Wiley, H. G.
Lee, C. Q.
A rigidly forced oscillation system for measuring dynamic-stability parameters in transonic and supersonic wind tunnels
NASA TN D-1231, 1962

66. Riley, D. R.
Bird, J. O.
Fisher, L. R.
Experimental determination of the aerodynamic derivatives arising from acceleration in sideslip for a triangular, a swept, and an unswept wing
NACA RM L55A07, 1955

67. Queijo, M. J.
Fletcher, H. S.
Marple, C. G.
Preliminary measurements of the aerodynamic yawing derivatives of a triangular, a swept, and an unswept wing performing pure yawing oscillations, with a description of the instrumentation employed
NACA RM L55L14, 1956

68. Queijo, M. J.
Jaquet, B. M.
Investigation of effects of geometric dihedral on low speed static stability and yawing characteristics of an untapered 45° sweptback-wing model of aspect ratio 2.61
NACA TN 1668, 1948

69. Bird, J. D.
Jaquet, B. M.
Cowan, J. W.
Effect of fuselage and tail surfaces on low-speed yawing characteristics of a swept-wing model as determined in curved-flow test section of the Langley Stability Tunnel
NACA TN 2483, 1951

70. Wright, B. R.
Brover, M. L.
Aerodynamic damping and oscillatory stability in pitch for a model of a typical subsonic jet-transport airplane
NASA TN D-3159, 1966

71. Kilgore, R. A.
Some transonic and supersonic dynamic stability characteristics of a variable-sweep-wing tactical fighter model
NASA TM X-2163, 1971

72. Kilgore, R. A.
Aerodynamic damping and oscillatory stability in pitch and yaw of a variable-sweep supersonic transport configuration at Mach numbers from 0.40 to 1.80
NASA TM X-2164, 1971

73. Kilgore, R. A.
Adcock, J. B.
Supersonic aerodynamic damping and oscillatory stability in pitch and yaw for a model of a variable-sweep fighter airplane with twin vertical tails
NASA TM X-2555, 1972

74. Schiff, L. B.
Tobak, M.
Results from a new wind-tunnel apparatus for studying coning and spinning motions of bodies of revolution
AIAA J. Vol. 8, No. 11, pp. 1953-1957, 1970

75. Beam, B. H.
A wind-tunnel test technique for measuring the dynamic rotary stability derivatives including the cross-derivatives at high Mach numbers
NACA TN 3347, 1955 (also NACA Rep.1258)

76. Beam, B. H.
Reed, V. D.
Lopez, A. E.
Wind-tunnel measurements at subsonic speeds of the static and dynamic rotary stability derivatives of a triangular-wing airplane model having a triangular vertical tail
NACA RM A55A28, 1955

77. Beam, B. H.
Endicott, K. C.
Wind-tunnel data on the longitudinal and lateral-directional rotary derivatives of a straight-wing, research airplane configuration at Mach numbers from 2.5 to 3.5
NACA RM A58A14, 1958

78. Tunnell, P. J.
Latham, E. A.
The static and dynamic rotary stability derivatives of a model of the X-15 research airplane at Mach numbers from 1.55 to 3.50
NASA Memo 12-23-58A, 1959

79. Lessing, H. C.
Butler, J. K.
Wind-tunnel investigation at subsonic and supersonic speeds of the static and dynamic stability derivatives of an airplane model with an unswept wing and a high horizontal tail
NASA Memo 6-5-59A, 1959

80. Tunnell, P. J.
The static and dynamic stability derivatives of a blunt half-cone entry configuration at Mach numbers from 0.70 to 3.50
NASA TM X-577, 1961

81. Lukasiewicz, J.
The need for developing a high Reynolds number transonic wind tunnel in the U.S.
Astronautics and Aeronautics, pp. 64-70, April 1971

82. Lukasiewicz, J. (Ed.)
Aerodynamic test simulation: lessons from the past and future prospects
AGARD Report 603, 1972

APPENDIX 1

ORGANIZATIONS AND PERSONS VISITED

(main contacts underlined)

1. NASA Ames Research Center

B. Beam
D. Ciffone
S. Doiguchi
K. Endicott
D. Englebert
W. McNeill
G. Malcolm
R. Nysmith
E. Perkins
(V. Peterson)
L. Schiff
F. Steinle
M. Tobak

2. Air Force Flight Dynamics Laboratory

T. Cord
D. Eckholdt
D. Hoak
V. Hoehne
J. Jenkins
G. Kurylowich
R. Nelson
R. Quaglieri
R. Schwarz
F. Thomas
R. Woodcock

3. NASA Manned Spacecraft Center

J. Gamble
E. Hillje
J. Klinar
B. Roberts
J. Young

4. ARO, Inc., Propulsion Wind Tunnel Facility

R. Carlton
M. Clermont
H. DuBose
M. Pindzola
L. Ring
T. Shadow

5. ARO, Inc., von Karman Gas Dynamics Facility

C. Schueler
J. Uselton
L. Ward
J. Whitfield

6. NASA Langley Research Center

(a) Low-Speed Aircraft Division

J. Bowman
J. Chambers
S. Grafton
J. Hassell, Jr.

(b) High-Speed Aircraft Division

J. Adcock
H. Wiley

(c) Space Systems Division

D. Freeman
A. Henderson, Jr.
B. Henry, Jr.

7. Naval Air System Command

T. Lawrence
R. Siewert

APPENDIX 2

Dear

I have been asked by NASA to make a brief survey of the capabilities in the USA and Canada for conducting dynamic stability tests. I would therefore greatly appreciate your kind cooperation in filling in the enclosed simple questionnaire, and returning it, at your earliest convenience, to me at

National Aeronautical Establishment,
Ottawa, Ontario, Canada
K1A 0R6

Please fill in one sheet for each wind tunnel (low speed to hypersonic) that is equipped for dynamic stability experiments. The field for each derivative is divided into three squares. Please insert the maximum angle of attack into the first square, the maximum sideslip angle into the second and the coded information about the method, apparatus and "special capabilities and remarks" into the third. Unless otherwise indicated under remarks, it will be assumed that the experiment utilizes an oscillatory, small-amplitude motion, and that the maximum angles of attack and sideslip can be attained at the same time. Please use short descriptive titles for the method(s) and apparatus(es). Examples of special capabilities and remarks include capabilities for considering effects of mass addition, ablation, simulated jet exhaust, propeller rotation, BLC, ground interaction, continuous rotation etc. Capabilities for obtaining cross-derivatives and testing at high angles of attack are of particular interest.

Please include references by number and attach a list of references. References to STA Proceedings will not be reproduced but please give them anyway, for my information. Please call me at (613) 993-2395 if there are any questions. Your cooperation will be greatly appreciated.

Yours sincerely

KOR/pm
encl.

K. Orlik-Rückemann

QUESTIONNAIRE
DYNAMIC STABILITY TEST EQUIPMENT

APPENDIX 2

Organization: Location:

Cognizant Person:

Wind Tunnel: Ref:

Mach Number Range: Re/ft.:
(or wind speed range)

Typical Aircraft Model Length: ft.

Dynamic Derivatives due to / of	Pitching			Yawing			Rolling			Vertical Acceleration		
Pitching moment												
Yawing moment												
Rolling moment												
Lift Force												
Side Force												

Methods: 1. Ref:

2.

3.

Apparatus: A.

B.

C.

Special Capabilities and Remarks a.

b.

c.

d.

Example: 20 | 10 | 2Ac at the intersection of the row "rolling moment" with the column "yawing" indicates a capability for measuring the derivative C_{ℓ_r} at a max. angle of attack of 20°, max. sideslip angle of 10°, using method 2, apparatus A and special capabilities and remarks c.

APPENDIX 3

ORGANIZATIONS COVERED BY PRESENT SURVEY

Abbrev.	Organization	Location	Cognizant Person	Dyn Stab Equipm	Ret'd Question
ARL	Aerospace Research Laboratories	WPAFB	E.G. Johnson	x	x
Boeing	The Boeing Company	Seattle		-	-
BRL	Ballistic Research Laboratories	Aberdeen	K. Opalka	x	x
CAL	Calspan Corporation	Buffalo	R.W. Cotter	x	x
Convair	GD Convair Aerospace Division	San Diego	D.P. Cumming	x	x
Convair	GD Convair Aerospace Division	FT. Worth	A.P. Madison	-	x
FluiDyne	FluiDyne Engineering Corporation	Minneapolis	J. Holdhusen	x	x
Grumman	Grumman Aerospace Corporation	Bethpage	W.J. Gander	-	x
JPL	Jet Propulsion Laboratory	Pasadena	P. Jaffe	x	x
LCC	Lockheed-California Company	Burbank	B. Robinson	-	x
LGC	Lockheed-Georgia Company	Marietta		-	-
Martin	Martin Marietta Corporation	Denver	S. Steinberg	-	x
MDE	McDonnell Douglas Corporation	El Segundo		-	-
MDS	McDonnell Douglas Corporation	St. Louis	F.M. Keyes	-	x
MIT	MIT Aerophysics Laboratory	Cambridge	C. Haldeman	x	x
NAE	National Aeronautical Establishment	Ottawa	K.J. Orlik-Rückemann	x	x
NAR	North American Rockwell Corporation	Los Angeles	G.M. Stone, Jr.	-	x
NASA-ARC	NASA Ames Research Center	Moffett Field	G. Malcolm	x	x
NASA-LRC LS	NASA Langley Research Center Low Speed Aircraft Division	Hampton	J.R. Chambers	x	x
NASA-LRC HS	NASA Langley Research Center High Speed Aircraft Division	Hampton	H.G. Wiley	x	x

APPENDIX 3 (concluded)

ORGANIZATIONS COVERED BY PRESENT SURVEY

Abbrev.	Organization	Location	Cognizant Person	Dyn Stab Equipm	Ret'd Question.
NASA-MSFC	NASA Marshall Space Flight Center	Huntsville	A.R. Felix	-	-
NOL	U.S. Naval Ordnance Laboratory	Silver Springs	S.M. Hastings	x	x
Notre Dame	University of Notre Dame	Notre Dame	C.W. Ingram	x	x
Northrop	Northrop Corporation	Hawthorne	P.F. Jensen	-	x
NSRDC	Naval Ship R&D Center	Washington	S.M. Gottlieb	x	x
PWT	ARO, Inc., Propulsion Wind Tunnel	Tullahoma	H.C. DuBose	x	x
Sandia	Sandia Corporation	Albuquerque	C.W. Peterson	x	x
VAC	Vought Aeronautics Company	Dallas	J.M. Cooksey	x	x
VKF	ARO, Inc., von Karman Gas Dynamics Facility	Tullahoma	J.C. Uselton	x	x

QUESTIONNAIRE

DYNAMIC STABILITY TEST EQUIPMENT

APPENDIX 4a

Organization: JPL - CALTECH

Location: PASADENA, CA

Cognizant Person: Peter Jaffe/Gil Herrera

Wind Tunnel: 21 in. Hypersonic Wind Tunnel

Ref: JPL TM33-335

Mach Number Range: 4-10
(or wind speed range)

Re/ft.: $1\text{-}3\times10^6$ (max)
Min 1/10 max

Typical ~~Axxexxaxk~~ Model ~~Length~~: 0.05-0.3 ft. Diam.

Dynamic Derivatives / due to of	Pitching			Yawing			Rolling			Vertical Acceleration		
Pitching moment	90 / 90		1Aa-d / 1Ba-d									
Yawing moment												
Rolling moment												
Lift Force												
Side Force												

Pitching Moment 120 - 2C

Methods: 1. Free-Flight } Both are unrestrained (except aerodynamically) free-oscillation techniques
2. Gas-Bearing }
3.

Ref:
AGARDogrpah 113
JPL TR 32-544
JPL TR 32-1012
JPL TR 32-1159
AIAA Paper 71-265

Apparatus: A. Gun Launch

B. Wire-Release

C. One-dim. free-oscillation gas bearing

Special Capabilities and Remarks

a. Pitch amplitude can be closely controlled

b. Models can be delicately constructed to emphasize particular data being obtained.

c. Up to 500 pictures can be obtained of completely unrestrained 6-deg. of freedom motion.

d. Model wall temperature can be controlled down to $T_w/T_\infty \sim$ unity.

Example: | 20 | 10 | 2Ac | at the intersection of the row "rolling moment" with the column "yawing" indicates a capability for measuring the derivative C_{ℓ_r} at a max. angle of attack of 20°, max. sideslip angle of 10°, using method 2, apparatus A and special capabilities and remarks c.

QUESTIONNAIRE

DYNAMIC STABILITY TEST EQUIPMENT

APPENDIX 4b

Organization: JPL - CALTECH

Location: PASADENA, CA

Cognizant Person: Peter Jaffe/Gil Herrera

Wind Tunnel: 20 in. Supersonic Wind Tunnel

Ref: JPL TM33-335

Mach Number Range: 0.3-0.8 and 1.2-4.8 (or wind speed range)

Re/ft_ℓ: $3\text{-}6 \times 10^6$ (max.) Min.: 1/30 of max.

Typical ~~Aixxraft~~ Model ~~Length~~ Diam.: 0.05-0.3 ft.

Dynamic Derivatives / due to of	Pitching			Yawing			Rolling			Vertical Acceleration		
Pitching moment	180 180		1Aacde 1Bbec									
Yawing moment												
Rolling moment												
Lift Force												
Side Force												

Pitching Moment 120 - 2c

Methods: 1. Free-Flight
2. Gas Bearing (one-dim)
3.

} Both are unrestrained (except aerodynamically) free oscillation techniques

Ref:
AGARDograph 113
JPL TR 32-544
JPL TR 32-1012
JPL TR 32-1159
AIAA Paper 72-983
AIAA Paper 71-265

Apparatus: A. Gun-Launch with Spin Head

B. Wire-Release

C. One-dim. free-oscillation gas bearing

Special Capabilities and Remarks

a. Spin-Rate and Yaw/Pitch amplitudes can be closely controlled.
b. Initial high angle-of-attack can be precisely set.
c. Models can be delicately constructed to emphasize data being obtained.
d. Up to 500 pictures can be obtained of completely unrestrained 6-deg. of freedom motion.
e. Model wall temperature can be controlled down to $T_w/T_\infty \sim$ unity.

*Note: The free-flight technique can be used in many other wind tunnels by the JPL staff.

Example: 20 | 10 | 2Ac at the intersection of the row "rolling moment" with the column "yawing" indicates a capability for measuring the derivative C_{ℓ_r} at a max. angle of attack of 20°, max. sideslip angle of 10°, using method 2, apparatus A and special capabilities and remarks c.

QUESTIONNAIRE

DYNAMIC STABILITY TEST EQUIPMENT APPENDIX 5

Organization: Naval Ordnance Laboratory Location: White Oak, Maryland

Cognizant Person: Mr. S. M. Hastings

Wind Tunnel: Hypersonic Tunnel (NOL Tunnel No. 8) Ref:

Mach Number Range: 5-10 (or wind speed range) Re/ft.: 5×10^7 max

Typical Aircraft Model Length: 2 ft.

Dynamic Derivatives / of due to	Pitching			Yawing			Rolling			Vertical Acceleration		
Pitching moment	15	1	3D, 4c, 1C, 2Aa, 2Ba									
Yawing moment				1	15	3D, 4c, 1C, 2Ab, 2Bb	15	0	6F			
Rolling moment							15	1	5E			
Lift Force												
Side Force							15	0	6F			

Methods: 1. Small amplitude free oscillation Ref:

2. Large amplitude free oscillation

3. Small amplitude forced oscillation
4. Free flight
5. Free decay 6. Magnus loads measurement

Apparatus: A. Ball bearing pivot (1 DOF)

B. Spherical Air bearing pivot (3DOF)

C. Flexure Pivot (1 DOF Torsion Rod and Crossed Flexure)
D. Internally driven forced oscillation balance (1 DOF)
E. Roll-damping balance F. Magnus balance

Special Capabilities and Remarks
a. Maximum angle of attack indicates pitch oscillation amplitude for this method.
b. Maximum sideslip angle indicates yaw oscillation amplitude for this method.
c. Nonlinear data-reduction capability
d.

Example: 20 | 10 | 2Ac at the intersection of the row "rolling moment" with the column "yawing" indicates a capability for measuring the derivative C_{lr} at a max. angle of attack of 20°, max. sideslip angle of 10°, using method 2, apparatus A and special capabilities and remarks c.

APPENDIX 6

AEDC DYNAMIC STABILITY MECHANISM SUMMARY

Mechanism	Max Normal Force	Applicable Tunnels								
		Transonic			Supersonic			Hypersonic		
	Tunnel	1T	4T	16T	16S	A	D	B	C	F
	Test Sect. Diam	1	0.4 - 1.3	16	16	3	1	4	4	2 - 9
	M_∞	0.2 - 1.5	1.6, 2.0	0.2 - 1.6	1.5 - 4.8	1.5 - 5	1.5 - 5.	6, 8	10	8.22
Pitch ($C_{m_q} + C_{m_{\dot{\alpha}}}$) and Yaw ($C_{n_r} - C_{n_{\dot{\beta}}}$) Damping										
Forced Oscillation										
VKF-1A	410		x	x	x	x				
VKF-1B high load, tapered sting	1200		x	x	x	x		x	x	
VKF-1C (low mass flow capability)	550		x	x	x	x		x	x	
PWT-16 e.g. nose blowing	8000			x	x					
PWT-4T being calibrated	600		x							
Free Oscillation										
VKF-2A 3-in gas bearing	300		x	x	x	x		x	x	
VKF-2B 1-in gas bearing	80		x			x	x	x	x	
VKF-2C high α sting	120									
tapered sting	500		x			x		x	x	
VKF-2D Tunnel D	120						x			
VKF-2F Tunnel F	500									x
PWT-16Ft	4500			x	x					
PWT-1T	100	x								
PWT-1T wall mounted; half plane	80	x								
Roll Damping (Cl_p)										
Forced Oscillation —										
VKF-1D — ($C_{n_p}, C_{Y_p}, C_{l_p}$)	1200		x	x	x	x		x	x	
PWT-16T in Design	4000			x	x					
Free Decay (Spinning Projectile)										
VKF-2E gas bearing	350		x	x	x	x		x	x	
Three Degree of Freedom										
VKF-3A spherical gas bearing	60		x	x	x	x		x	x	
Free Flight										
VKF-Free Flight Launcher	-					x		x	x	

APPENDIX 7

DYNAMIC STABILITY BALANCES

NASA Langley Research Center - High Speed Aircraft Division

Balance	Mode	Static Load Limits, pounds or inch-pounds						Tunnels	Status
		Normal	Axial	Pitch	Roll	Yaw	Side		
GA-16	q,n	2000	2000	6000	300	6000	2000	A,B,C	C
GA-14	"	600	1600	6400	100	6400	600	"	C
DS-02P	"	400	800	1200	200	200	400	C	B
DS-03P	"	150	1000	400	200	250	250	A,B,C	B
DS-01R	ℓ	1000	700	3000	500	250	250	A,B	C
DS-05R	ℓ	1000	700	3000	500	150	150	A,B,C	A

Modes

- q - Pitching
- n - Yawing
- ℓ - Rolling

Tunnels

- A - Langley 7x10 Foot High Speed
- B - Langley 8-Foot Transonic
- C - Langley Unitary Plan Wind Tunnels

Status

- A - Constructed
- B - Gaged
- C - Operational

TABLE 1

HYPERVELOCITY AND HYPERSONIC WIND TUNNELS EQUIPPED FOR DYNAMIC STABILITY EXPERIMENTS

Organization Location Facility Name	Type of Facility	Test Section Size	Mach Range	Reynolds Number per ft x 10^{-6}	Total temp, °R	Dynamic Pressure psf	Time, sec	Page in Ref 30
ARL WPAFB 20-inch HWT	blowdown to vacuum	20" diam	12,14	0.5	500-2500	20-140	20-300	3-16
FluiDyne Minneapolis 20-inch HWT	blowdown to vacuum	20" diam (free jet)	12,14	0.08-1	1200-4000		60	3-34
JPL Pasadena 21 inch HWT	variable density, continuous	25"x20"	4-10	0.2-3	560-1810	13-460	Cont.	3-78
NAE Ottawa Helium HWT	blowdown to vacuum	11" diam	11,18	2-19	530-640	190-2000	5-30	-
NOL Silver Springs Hypervelocity Research WT	blowdown to exhaust system	18" diam	12,17 (N_2)	0.1-5	2000-4000		240-cont.	3-112
NOL Silver Springs Hypersonic, No.8	blowdown to atmosphere or exhaust system	18" diam	5-10	0.3-50	700-2000	50-7000	30-cont.	3-112
NOL Silver Springs Hypervelocity WT	blowdown to vacuum	60" diam	10-20	1.3-20	1850-5000		1-4	-

TABLE 1 (concluded)

Organization Location Facility Name	Type of Facility	Test Section Size	Mach Range	Reynolds Number per ft x 10^{-6}	Total temp, °R	Dynamic Pressure, psf	Time, sec	Page in Ref 30
Sandia Albuquerque 12 inch HWT	blowdown to vacuum	18" diam (free jet)	5,7, 11,14	0.1-4	640-3000	85-720	45	3-122
VAC Dallas Hypervelocity WT	arc fired	13" diam closed jet	10-20	0.1-12	2700-8100	16-2000	0.03-0.3	3-48
VKF Tullahoma HWT B	recycling variable density continuous	50" diam	6,8	0.3-4.7	850-1350	43-590	cont	-
VKF Tullahoma HWT C	recycling variable density continuous	50" diam	10,12	0.3-2.2	1910-2350	43-400	cont	-
VKF Tullahoma HWT F	arc driven	54" diam	8,14 10-19	0.1-22	2000-7200	14-4500	0.1	-

TABLE 2

SUPERSONIC WIND TUNNELS EQUIPPED FOR DYNAMIC STABILITY EXPERIMENTS

(for "trisonic" wind tunnels - see also TABLE 3)

Organization Location Facility Name	Type of Facility	Test Section Size	Mach Range	Reynolds Number per ft x 10^{-6}	Total temp, °R	Dynamic Pressure psf	Time, sec	Page in Ref 30
BRL Aberdeen SWT no.1	variable density, continuous	1.25'x1.08'	1.5-5	0.5-8.5	540-590	36-1800	cont	2-6
BRL Aberdeen SWT no.3	variable density, continuous	1.67'x1.25'	1.3-4.5	1.4-8.5	540-590	140-1800	cont	2-8
JPL Pasadena 20 inch SWT	continuous	1.67x1.5'	1.2-4.8	0.1-6	520-620		cont	-
MIT Cambridge Gas dynamic WT		0.3'x0.3'	4.2-6.2	0.3-2				-
NASA-LRC Hampton Unitary Plan WT	variable density, continuous	4'x4'	1.47-4.63	0.4-7.8	610-635	83-1550	cont	2-58
NOL Silver Springs Supersonic WT no.2	recycling or blowdown, variable density	1.3'x1.3'	1.5-5	.05-20	530-635		60-300	2-66
Notre Dame Notre Dame 5 inch SWT	suction atmosphere to vacuum	5"x5"	1.5	4.7	ambient		cont	-
NSRDC Washington 18 inch SWT	blowdown to vacuum	1.5'x1.5'	1.56-4.5	1-5	ambient	58-805	26 max	2-76

TABLE 2(concluded)

Organization Location Facility Name	Type of Facility	Test Section Size	Mach Range	Reynolds Number per ft x 10^{-6}	Total temp, °R	Dynamic Pressure psf	Time, sec	Page in Ref 30
PWT Tullahoma 16S	variable density, continuous	16'x16'	1.5-4.8	0.1-2.5	560-1110	50-550	cont	-
VKF Tullahoma SWT A	variable density, continuous	3.3'x3.3'	1.5-5	0.3-9.2	530-750	49-1780	cont	-
VKF Tullahoma SWT D	blowdown	1'x1'	1.5-5	0.26-16	540	37-3100	300	-

TABLE 3

TRANSONIC WIND TUNNELS EQUIPPED FOR DYNAMIC STABILITY EXPERIMENTS

(this table includes the so called "trisonic" wind tunnels)

Organization Location Facility Name	Type of Facility	Test Section Size	Mach Range	Reynolds Number per ft x 10^{-6}	Total temp, °R	Dynamic Pressure psf	Time, sec	Page in Ref 30
CAL Buffalo 8 Foot Transonic	variable density, continuous	8'x8'	0-1.3	0.7-7	560-615	50-800	cont.	2-14
Convair San Diego High Speed WT	blowdown to atmosphere	4'x4'	0.5-5	5-23	560	1000-2500	45-90	2-18
NAE Ottawa 30 inch WT	suction atmosphere to vacuum	2.5'x1.2'	0.3-2	2-4.7	540	200-870	13	-
NASA-ARC Moffett Field 6x6 ft supersonic	variable density, continuous	6'x6'	0.6-2.2	0.5-5	580	200-1000	cont.	2-44
NASA-LRC Hampton 8 Foot Transonic Pressure WT	variable density, continuous	7.1'x7.1'	0.2-1.2	0.1-6	580	60-1260	cont.	2-48
NSRDC Washington 7x10 ft transonic	variable density, continuous	7'x10'	0.4-1.15	0.7-5.6	610	50-950	cont.	2-78
PWT Tullahoma 16 T	variable density, continuous	16'x16'	0.2-1.6	0.1-7.5	410-620	25-1280	cont.	-
PWT Tullahoma 4 T	variable density, continuous	4'x4'	0.1-1.3, 1.6,2.0	0.2-7.7		20-1600	cont.	-

TABLE 3(concluded)

Organization Location Facility Name	Type of Facility	Test Section Size	Mach Range	Reynolds Number per ft x 10^{-6}	Total temp, °R	Dynamic Pressure psf	Time, sec	Page in Ref 30
PWT Tullahoma 1 T	no-return continuous	1'x1'	0.2-1.5	3.5-5.3	610-640	420-1200	cont.	-
Sandia Albuquerque 12-inch transonic	blowdown	1'x1'	0.7-2.5	4-10	540		15-60	-
VAC Dallas 4x4 ft HSWT	blowdown to atmosphere	4'x4'	0.4-5	4-38	560	150-5000	40-120	2-28

TABLE 4

SUBSONIC WIND TUNNELS EQUIPPED FOR DYNAMIC STABILITY EXPERIMENTS

(for "trisonic" wind tunnels - see also Table 3)

Organization Location Facility Name	Type of Facility	Test Section Size	Mach Range	Reynolds Number per ft x 10^{-6}	Total temp, °R	Dynamic Pressure psf	Time, sec	Page in Ref 30
NASA-LRC Hampton Full Scale Tunnel	closed circuit, open throat, continuous	30'x60'	0-0.1	0-1	540	0-30	cont.	1-36
NASA-LRC Hampton HS 7x10 Foot Tunnel	closed circuit, continuous	6.6'x9.6'	0.2-.85	0.1-3.2	490-620	200-750	cont.	1-40
Notre Dame Notre Dame Subsonic W.T.	open circuit	2'x2'	0-0.18	0-1.3	540		cont.	-
NSRDC Washington 8x10 Foot Subsonic W.T.	closed circuit, continuous	8'x10'	0-0.2	0-1.6	576	0-90	cont	1-50
VAC Dallas 7x10 Foot Low Speed W.T.	closed circuit, continuous	7'x10'	0.02-0.36	0.06-2.1	540	2-135	cont.	1-20

TABLE 5a

FACILITIES FOR MEASURING PITCH AND YAW DAMPING (HYPERSONIC)

Wind Tunnel	Mach Number	Reynolds Number x 10^{-6} (Model Length)	Method	Apparatus	Pitch Damping $\alpha_{max}, \beta_{max}$ deg.		Yaw Damping $\alpha_{max}, \beta_{max}$ deg.		Remarks	Ref.
ARL 20 inch HWT	12,14	0.5 (1 ft)	Free Osc.	Torsion Bar Flexures	30	6	6	30		31
FluiDyne 20 inch HWT	11,14	0.8-1 (1 ft)	Free Osc.	Air Bearing, Aft or Side Strut	25	0	0	25	Mass Addition by Ablation or Phase Blowing	32 33
JPL 21 inch HWT	4-10	0.02-0.1 (0.05 ft dia)	Free Flight	Gun Launch or Wire Release	90	0	-	-	No Aircraft Models (yet); See Appendix 4a	35 to 39
JPL 21 inch HWT	4-10	0.1-0.6 (0.3 ft dia)	Free Osc.	1 DOF Gas Bearing	120	0	-	-		
NAE Helium HWT	11,18	1.6-16 (0.8 ft)	Free or Forced Osc.	Half Model	25	0	-	-	Also Full Model at $\alpha = 0^{\circ}$	34
NOL Hypervelocity Research WT	12,17	0.1-5 (1 ft)	Free Osc.	1 DOF Flexure	10	0	0	10	Optical Motion Sensor	
NOL Hypersonic, No 8	5-10	0.6-100 (2 ft)	Free Osc.-Flexure Pivot Forced Osc.-Internal Drive Free Flight-Nonlinear Data		15	1	1	15	See Appendix 5	40 to 42
			Free Osc.-1 DOF Ball Bearing Free Osc.-3 DOF Air Bearing		Ampl. ±15		Ampl. ±15			

TABLE 5a (concluded)

Wind Tunnel	Mach Number	Reynolds Number x 10^{-6} (Model Length)	Method	Apparatus	Pitch Damping $\alpha_{max}, \beta_{max}$ deg.		Yaw Damping $\alpha_{max}, \beta_{max}$ deg.		Remarks	Ref.
NOL Hypervelocity WT	10-20	9-140 (7 ft)	Free Osc.	1 DOF Flexure	10	0	0	10		43
Sandia 12 inch HWT	5, 7, 11, 14	0.1-4 (1 ft)	Free Osc.	Strap Rig, or Gas Bearing	15	0	-	-		44
VAC Hypervelocity WT	10-20	0.05-6 (0.5 ft)	Free Osc.	Flexure Pivot	20	10	10	20	Phased Oscillatory Mass Addition	45 to 48
VKF HWT B	6, 8	1.2-21 (4 ft)	Free or Forced Oscillation	Flexure Pivot or Gas Bearing	15	0	0	15		
VKF HWT C	10, 12	1.2-10 (4 ft)	Free or Forced Oscillation	Flexure Pivot or Gas Bearing	15	0	0	15	See Appendix 6	29
VKF HWT F	8, 14 10-19	0.4-90 (4 ft)	Free Osc.	Flexure Pivot	15	0	0	15		

TABLE 5b

FACILITIES FOR MEASURING PITCH AND YAW DAMPING (SUPERSONIC)

Wind Tunnel	Mach Number	Reynolds Number x 10^{-6} (Model Length)	Method	Apparatus	Pitch Damping $\alpha_{max}, \beta_{max}$ deg.		Yaw Damping $\alpha_{max}, \beta_{max}$ deg.		Remarks	Ref.
BRL SWT No 1	1.5-5	0.5-8.5 (1.0 ft)	Free Osc.	Flexure Pivot	15	3.5	-	-		49
BRL SWT No 3	1.3-4.5	2-12 (1.5 ft)	Free Osc.	Flexure Pivot	15	3.5	-	-		49
JPL 20 inch SWT	1.2-4.8	0.01-0.3 (0.05 ft dia)	Free Flight	Gun Launch or Wire Release	180	0	-	-	Spin Head; No Aircraft Models (yet); See Appendix 4b	35 to 39
JPL 20 inch SWT	1.2-4.8	0.03-1.8 (0.3 ft dia)	Free Osc.	1 DOF Gas Bearing	120	0	-	-		
MIT Gasdynamic WT	4.2,6.2	0.15-1 (6 in)	Free or Forced Osc.	Magnetic Balance	10	0	-	-	Under Development	
NASA-LRC Unitary Plan WT	1.5-4.6	1-20 (2.5 ft)	Forced Osc.	Eccentric Crank and Crosshead Electric Drive	25 (α and β cannot be obtained simultaneously)	25	25	25	See Appendix 7	50 51
NOL Supersonic WT No 2	1.5-5	0.1-30 (1.5 ft)	Free Osc.-Flexure Pivot Forced Osc.-Internal Drive Free Flight-Nonlinear Data		15	15	15	15	Remarks Similar to Appendix 5	42
			Free Osc.-1 DOF Ball Bearing		Ampl. ± 15		Ampl. ± 15			
			Free Osc.-3 DOF Air Bearing							

TABLE 5b (concluded)

Wind Tunnel	Mach Number	Reynolds Number x 10^{-6} (Model Length)	Method	Apparatus	Pitch Damping $\alpha_{max}, \beta_{max}$ deg.		Yaw Damping $\alpha_{max}, \beta_{max}$ deg.		Remarks	Ref.
Notre Dame 5 inch SWT	1.5-1.7	0.8 (2 in)	Free Osc.	3 DOF Ball Bearing	20	20	20	20	High Speed Camera Recording	
NSRDC 18 inch SWT	1.56-4.5	1.8-8.5 (1.75 ft)	Free Osc.		0	0	0	0		52
PWT 16S	1.5-4.8	0.4-10 (4 ft)*	Free or Forced Osc.	Flexure Pivot or Gas Bearing	15	0	0	15	Nose Blowing	
VKF SWT A	1.5-5	1-28 (3.3 ft)	Free or Forced Osc.	Flexure Pivot or Gas Bearing	15	0	0	15	See Appendix 6	29
VKF SWT D	1.5-5	0.3-16 (1 ft)	Free Osc.	Gas Bearing	15	0	0	15		

* could be increased

TABLE 5c

FACILITIES FOR MEASURING PITCH AND YAW DAMPING (TRANSONIC)

Wind Tunnel	Mach Number	Reynolds Number x 10^{-6} (Model Length)	Method	Apparatus	Pitch Damping $\alpha_{max}, \beta_{max}$ deg.		Yaw Damping $\alpha_{max}, \beta_{max}$ deg.		Remarks	Ref.
CAL 8 ft Transonic	0-1.3	14 (4 ft)	Forced Osc.	2 DOF Mech. Drive	10	0	0	20	Can Separate q and $\dot{\alpha}$ Derivatives	53
CAL 8 ft Transonic	0-1.3	14 (4 ft)	Free Osc.	Pivot	20	10	10	20	Adapters for Higher Angles	
NAE 30 inch WT	0.3-2	2-3 (0.6 ft)	Free or Forced Osc.	Flexures, Internal or External Drive	20	10	10	20	Also Half Model, $\alpha < 25°$	54 55
NASA-LRC 8 ft Transonic Pressure WT	0.2-1.2	20 (3 ft)	Forced Osc.	Eccentric Crank and Crosshead Elec. Drive	22	22	22	22	See Appendix 7	50 51
					(α and β cannot be obtained simultaneously)					
NSRDC 7 x 10 ft Transonic	0.4-1.15	2-16 (3 ft)	Forced Osc.	1 DOF	20	15	15	20		56

TABLE 5c (concluded)

Wind Tunnel	Mach Number	Reynolds Number x 10^{-6} (Model Length)	Method	Apparatus	Pitch Damping $\alpha_{max}, \beta_{max}$ deg.		Yaw Damping $\alpha_{max}, \beta_{max}$ deg.		Remarks	Ref.
PWT 16T	0.2-1.6	0.4-30 (4 ft)*	Free or Forced Osc.	Flexure Pivot or Gas Bearing	15	0	0	15	Nose Blowing	
PWT 4T	0.1-1.3 1.6,2.0	0.8-30 (4 ft)	Free or Forced Osc.	Flexure Pivot or Gas Bearing	15	0	0	15	See Appendix 6	29
PWT 1T	0.2-1.5	3.5-5.3 (1 ft)	Free Osc.	Flexure Pivot also Half Model	15	0	0	15		
Sandia 12 inch Transonic	0.7-2.5	4-10 (1 ft)	Free Osc.	Strap Rig	15	0	-	-		44
VAC 4 x 4 ft HSWT	0.4-5.0	0.8-10 (2 ft)	Free Osc.	Flexure Pivot or Bearing	0	10	22	0	Cross-Rod or Sting	

* could be increased

TABLE 5d

FACILITIES FOR MEASURING PITCH AND YAW DAMPING (SUBSONIC)

Wind Tunnel	Mach Number	Reynolds Number x 10^{-6} (Model Length)	Method	Apparatus	Pitch Damping $\alpha_{max}, \beta_{max}$ deg.		Yaw Damping $\alpha_{max}, \beta_{max}$ deg.		Remarks	Ref.
NASA-LRC Full Scale Tunnel	0-0.1	5.6 (7 ft)	Forced Osc.	6-Comp. Balance	90	90	90	90	Amplitudes up to $\pm 30^{\circ}$ also Powered Models	11,12, 21,57, 58
NASA-LRC Full Scale Tunnel	0-0.1	5.6 (7 ft)	Continuous Rotation	Rotary Balance	30 to 90	± 10	30 to 90	± 10	Max rpm 200; Spin Radius up to 1 ft	
NASA-LRC HS 7x10 ft Tunnel	0.2-0.85	12 (3 ft)	Forced Osc.	Eccentric Crank and Crosshead Elec. Drive	22	22 (α and β cannot be obtained simultaneously)	22	22	See Appendix 7	50,51
Notre Dame Subsonic WT	0-0.18	1.3 (1 ft)	Free Osc.	3 DOF Ball Bearing	20	20	20	20	Model Motion Recorded	
NSRDC 8x10 ft Subsonic WT	0-0.2	4.8 (3 ft)	Forced Osc.	1 DOF	15	0	0	15	Ground Interaction	56
VAC 7x10 ft Low Speed WT	0.02-0.36	0.2-8 (4 ft)	Free Osc.	Bearing or Flexure Pivot	0	90	90	0	Cross-Rod or Sting	

TABLE 6

FACILITIES FOR MEASURING DERIVATIVES DUE TO ROLLING

Wind Tunnel	Mach Range	Reynolds Number x 10^{-6}	Model Length ft	Method	Apparatus	Derivatives	α_{max} deg.	β_{max} deg.	Ref.
ARL 20-inch HWT	12,14	0.5	1	Free Roll	Air Bearing	$C_{\ell p}$	15	0	60
CAL 8-ft Transonic	0-1.3	14	4	Free Spinning	Bearings	C_{np}, C_{Yp}	20	0	
Convair HSWT	0.5-5	20-92	4	Free Spinning Measure Roll Acceleration	Optical Roll Indicator	$C_{\ell p}$	23	0	
MIT Gasdynamics WT	4.2,6.2	0.15-1	0.5	Spin Down	Magnetic Balance	$C_{\ell p}$	10	0	
NAE 30-inch WT	0.3-2	2-3	0.6	Free or Forced Osc.	Elastic Suspension El.-Magn. Drive	$C_{\ell p}$	15	10	
NASA-LRC Full Scale Tunnel	0-0.1	5.6	7	Continuous Rotation	Rotary Balance 6-Comp.	$C_{np}, C_{\ell p}$ C_{Yp}, C_{Lp} C_{mp}	30 to 90	10	

TABLE 6 (continued)

Wind Tunnel	Mach Range	Reynolds Number x 10^{-6}	Model Length ft	Method	Apparatus	Derivatives	α_{max} deg.	β_{max} deg.	Ref.
NASA-LRC Full Scale Tunnel	0-0.1	5.6	7	Forced Osc.	6-Comp. Balance	C_{np}, $C_{\ell p}$ C_{Yp}, C_{Np} C_{mp}, C_{Ap}	$\pm$90	$\pm$90	11,12, 21,57, 58
NASA-LRC HS 7x10 ft Tunnel	0.2-0.85	12	3	Forced Osc.	Electric Drive via Eccentric Crank	C_{np}, $C_{\ell p}$	22*	22*	64
NASA-LRC HS 7x10 ft Tunnel	0.2-0.85	12	3	Continuous Rotation	Rotary Balance Hydraulic Drive	C_{np}, $C_{\ell p}$ C_{Yp}	25		62,63
NASA-LRC 8 ft Transonic Pressure WT	0.2-1.2	20	3	Forced Osc.	Electric Drive via Eccentric Crank	C_{np}, $C_{\ell p}$	22*	22*	64
NOL Supersonic WT No 2	1.5-5	0.1-30	1.5	Free Roll	Damping Balance	$C_{\ell p}$	15	15	42
				Continuous Roll	Magnus Balance	C_{np}, C_{Yp} C_{mp}, C_{Np}	15 0	0 15	61

* angles α and β cannot be obtained simultaneously

TABLE 6 (continued)

Wind Tunnel	Mach Range	Reynolds Number x 10^{-6}	Model Length ft	Method	Apparatus	Derivatives	α_{max} deg.	β_{max} deg.	Ref.
NOL Hypersonic Tunnel No 8	5-10	0.6-100	2	Free Roll	Damping Balance	$C_{\ell p}$	15	1	42
				Continuous Roll	Magnus Balance	C_{np}, C_{Yp}	15	0	61
Notre Dame 5-inch SWT	1.5	0.8	0.16	Free Motion 3 DOF	Motion Recording	$C_{\ell p}$, C_{np}(?)	20	20	
Notre Dame Subsonic WT	0-0.18	1.3	1						
PWT 4 T	0.1-1.3 1.6,2.0	0.2-7.7	4	Forced Osc.		$C_{\ell p}$, C_{np} C_{Yp}	15*	15*	
PWT 16 T	0.2-1.6	0.1-7.5	4	Free Decay		$C_{\ell p}$	15*	15*	
PWT 16 S	1.5-4.8	0.4-10	4**						

* angles α and β cannot be obtained simultaneously

** can be increased

TABLE 6 (concluded)

Wind Tunnel	Mach Range	Reynolds Number x 10^{-6}	Model Length ft	Method	Apparatus	Derivatives	α_{max} deg.	β_{max} deg.	Ref.
VAC 7x10 ft LSWT	0.02-0.36	0.2-8	4	Free or Steady Roll	6-Comp. Balance Air Turbine or Canted Fins	$C_{\ell p}$, C_{Yp}	90	30	
VAC 4x4 ft HSWT	0.4-5	0.8-10	2				22	10	
VKF SWT A	1.5-5	1.2-30	3.3	Forced Osc. or Free Decay		$C_{\ell p}$, C_{np} C_{Yp}	15	15	
VKF HWT B	6,8	1.2-21	4			$C_{\ell p}$	15	15	
VKF HWT C	10	1.2-10	4						

TABLE 7

FACILITIES FOR MEASURING OTHER DYNAMIC DERIVATIVES

Wind Tunnel	Mach Range	Reynolds Number x 10^{-6}	Model Length ft	Method and Apparatus	Derivatives	α_{max} deg.	β_{max} deg.	Ref.
CAL 8-foot Transonic	0-1.3	14	4	2 DOF Forced Osc.; q and $\dot{a}$ - Effects Separately Controlled	C_{mq}, $C_{m\dot{a}}$ C_{Nq}, $C_{N\dot{a}}$ C_{nr}, $C_{n\dot{\beta}}$ C_{Yq}, $C_{Y\dot{\beta}}$	10 0	0 20	53
MIT Gasdynamic WT	4.2,6.2	0.15-1	0.5	Free or Forced Osc. Magnetic Balance (under development)	$C_{m\dot{a}}$	10		
NASA-LRC Full Scale Tunnel	0-0.1	5.6	7	Continuous Rotation Rotary Balance	C_{nq}, $C_{\ell q}$ C_{Nq}, C_{Yq} C_{mr}, $C_{\ell r}$ C_{Nr}, C_{Yr}	30 to 90	±10	
NASA-LRC Full Scale Tunnel	0-0.1	5.6	7	Forced Oscillation 6-Comp. Balance	C_{nq}, $C_{\ell q}$ C_{Nq}, C_{Yq} C_{mr}, $C_{\ell r}$ C_{Nr}, C_{Yr} C_{Aq}, C_{Ar}	90	90	11,12 21,57 58

TABLE 7 (concluded)

Wind Tunnel	Mach Range	Reynolds Number x 10^{-6}	Model Length ft	Method and Apparatus	Derivatives	α_{max} deg.	β_{max} deg.	Ref.
NASA-LRC HS 7x10 ft Tunnel	0.2-0.85	12	3	Forced Oscillation Eccentric Crank and Crosshead Electric Drive	$C_{\ell r}$, C_{Nq}	22*	22*	
NASA-LRC Unitary Plan Wind Tunnels	1.5-4.6	1-20	2.5	Forced Oscillation Eccentric Crank and Crosshead Electric Drive	$C_{\ell r}$, C_{Nq}	25*	25*	
NASA-LRC 8 ft Transonic Pressure WT	0.2-1.2	20	3	Forced Oscillation Eccentric Crank and Crosshead Electric Drive	$C_{\ell r}$, C_{Nq}	25*	25*	
NAE 30 inch WT	0.3-2	2-3	0.6	Forced Oscillation; Electro-magnetic Drive; Cruciforms	C_{mr}, C_{nq} $C_{\ell r}$, $C_{\ell q}$	20	10	

* angles α and β cannot be obtained simultaneously

TABLE 8

NEEDS VERSUS CAPABILITIES

NEEDS			CAPABILITIES			
Mach Range	Angle of Attack deg.	Derivatives	Mach Range	Angle of Attack deg.	Derivatives	Tunnels with Highest Re
<0.6	≤20	$C_{mq}, C_{\ell p}, C_{nr}, C_{np}, C_{\ell r}$ $C_{m\dot{\alpha}}, C_{n\dot{\beta}}$	<0.6	≤22 (25) ≤10 (20?)	$C_{mq}, C_{\ell p}, C_{nr}, C_{np}, [C_{\ell r}]$ $C_{m\dot{\alpha}}, C_{n\dot{\beta}}$	NASA-LRC CAL
	20-50	$C_{mq}, C_{\ell p}, C_{nr}, C_{np}, C_{\ell r}$	≤0.1	≤90	$C_{mq}, C_{\ell p}, C_{nr}, C_{np}, [C_{\ell r}]$ also $C_n = f(rb/2V)$	NASA-LRC
	40-90	$C_{mq}, C_{\ell p}, C_{nr}, C_{np}, C_{\ell r}$, $= f(\Omega b/2V)$	<0.4	≤90	$C_{\ell p}$	VAC
0.4-2	≤20	$C_{mq}, C_{\ell p}, C_{nr}, C_{np}, C_{\ell r}$ $C^*_{m\dot{\alpha}}, C^*_{n\dot{\beta}}, C^*_{\ell\beta}$	0.2-1.2	≤22	$C_{mq}, C_{\ell p}, C_{nr}, C_{np}, [C_{\ell r}]$	NASA-LRC, (NSRDC)
			0.1-2	≤15	$C_{mq}, C_{\ell p}, C_{nr}, C_{np}$	PWT
			0-1.3	≤10	$C_{mq}, C_{nr}, C_{m\dot{\alpha}}, C_{n\dot{\beta}}$	CAL
			1.2-2	≤20	$C_{mq}, [C_{m\dot{\alpha}}]$	NAE
	20-50	$C_{mq}, C_{\ell p}, C_{nr}, C_{np}, C_{\ell r}$	0.2-0.85	≤25	$C_{\ell p}, C_{np}$	NASA-LRC
			1.5-2	≤25	C_{mq}, C_{nr}	NASA-LRC
			0.2-1.2	≤25	$[C_{\ell r}]$	NASA-LRC

TABLE 8 (concluded)

NEEDS			CAPABILITIES			
Mach Range	Angle of Attack deg.	Derivatives	Mach Range	Angle of Attack deg.	Derivatives	Tunnels with Highest Re
2-7	≤50	$C_{mq}, C_{\ell p}, C_{nr}, C^*_{np}, C^*_{\ell r}$	1.5-4.6	≤25	$C_{mq}, C_{nr}, [C_{\ell r}], [C_{\ell p}]$	NASA-LRC
			2	≤20	$[C_{\ell r}]$	NAE
			1.5-5	≤15	$C_{mq}, C_{\ell p}, C_{nr}, C_{np}$	NOL, VKF, PWT (Convair) (BRL)
			2-5	≤22	$C_{\ell p}$	VAC
≥5	≤55	$C_{mq}, C_{\ell p}, C_{nr}$	5-10	≤15	$C_{mq}, C_{\ell p}, C_{nr}$	NOL, VKF
			12-14(20)	≤15 (30)	$C_{mq}, C_{\ell p}, C_{nr}$	ARL, (NOL) (FluiDyne) (VAC), (VKF)

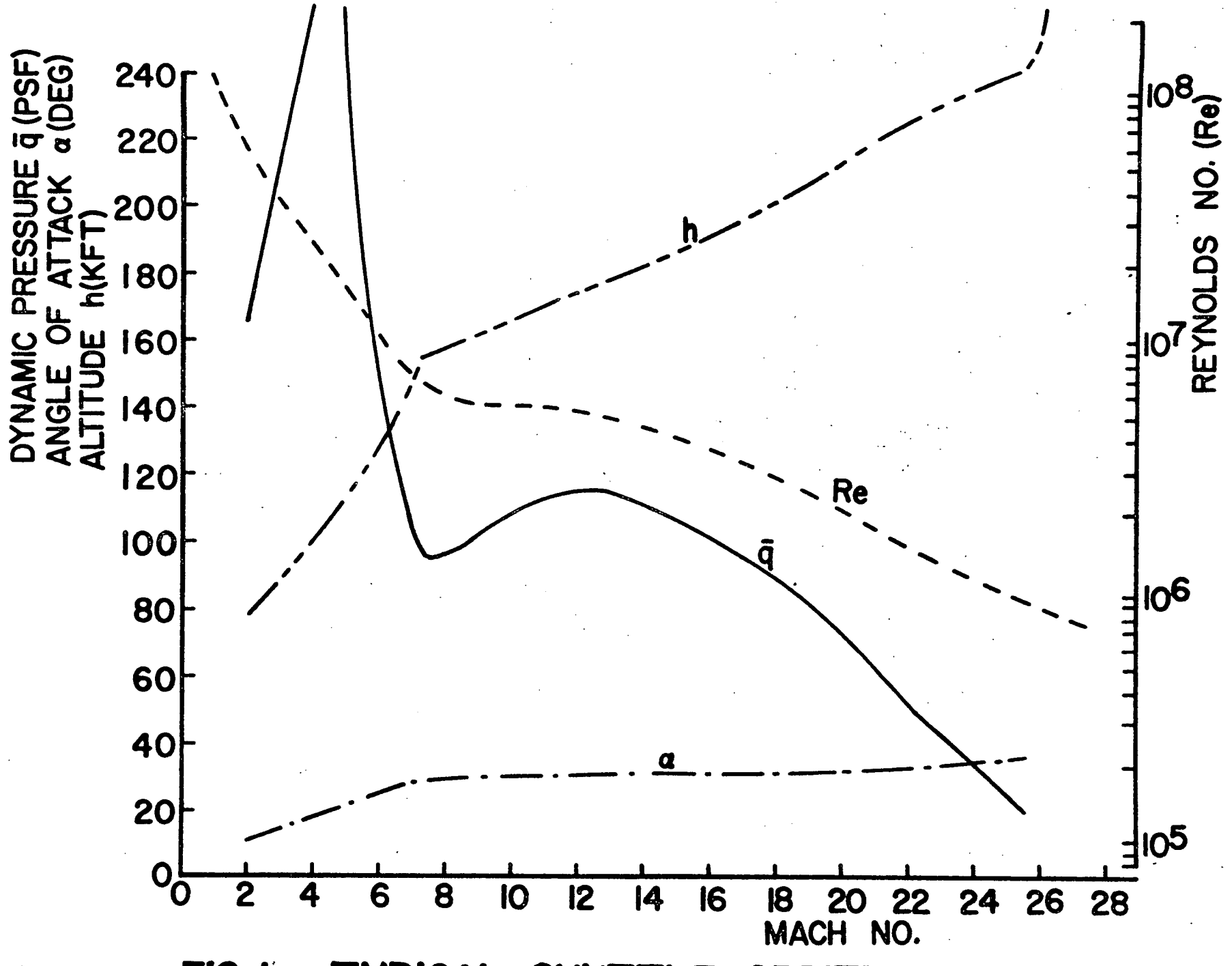

FIG 1 TYPICAL SHUTTLE ORBITER ENTRY TRAJECTORY

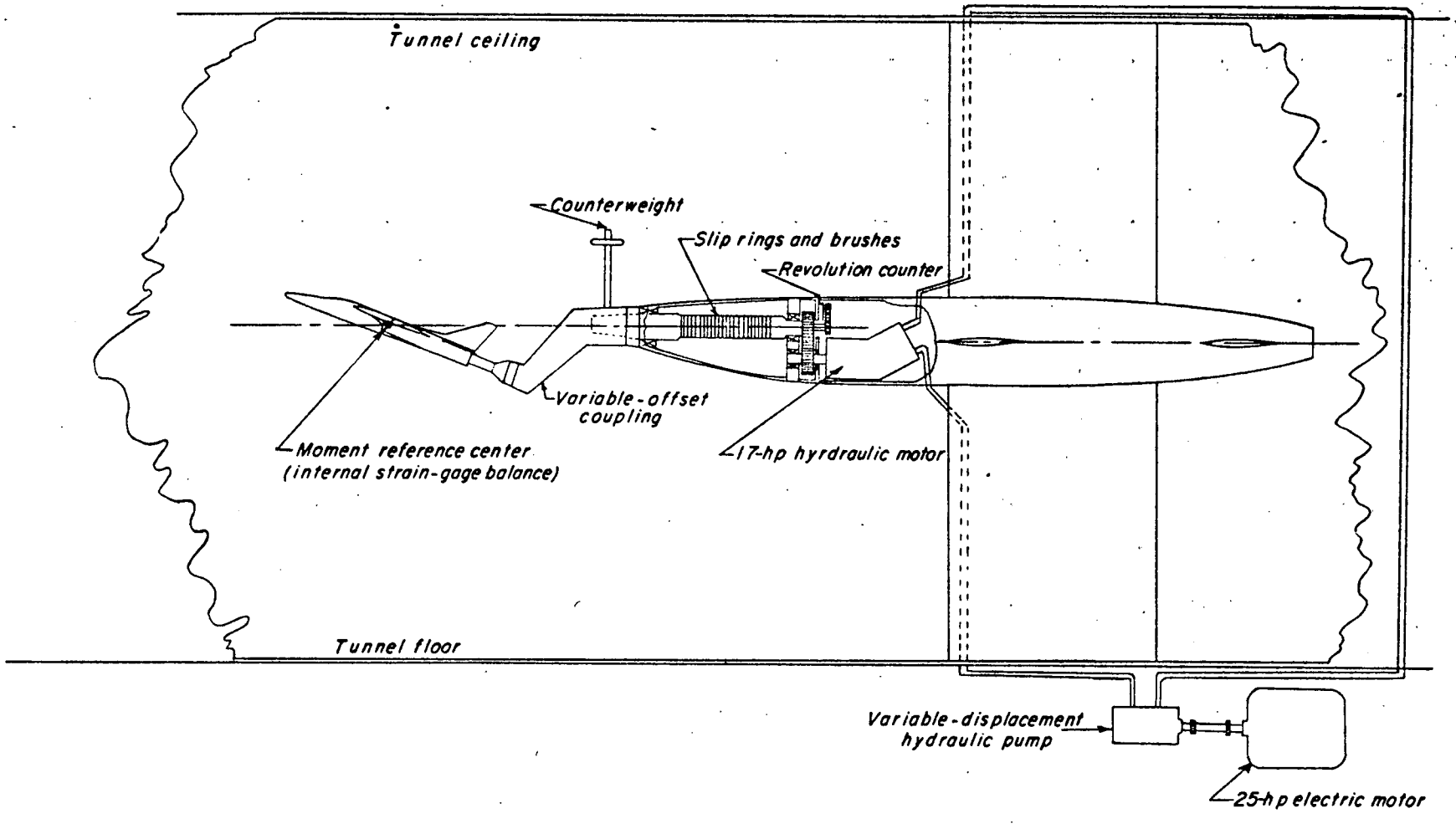

Fig. 2 Steady-state Forced-roll Apparatus
7x10 Foot High Speed Tunnel
NASA - LRC

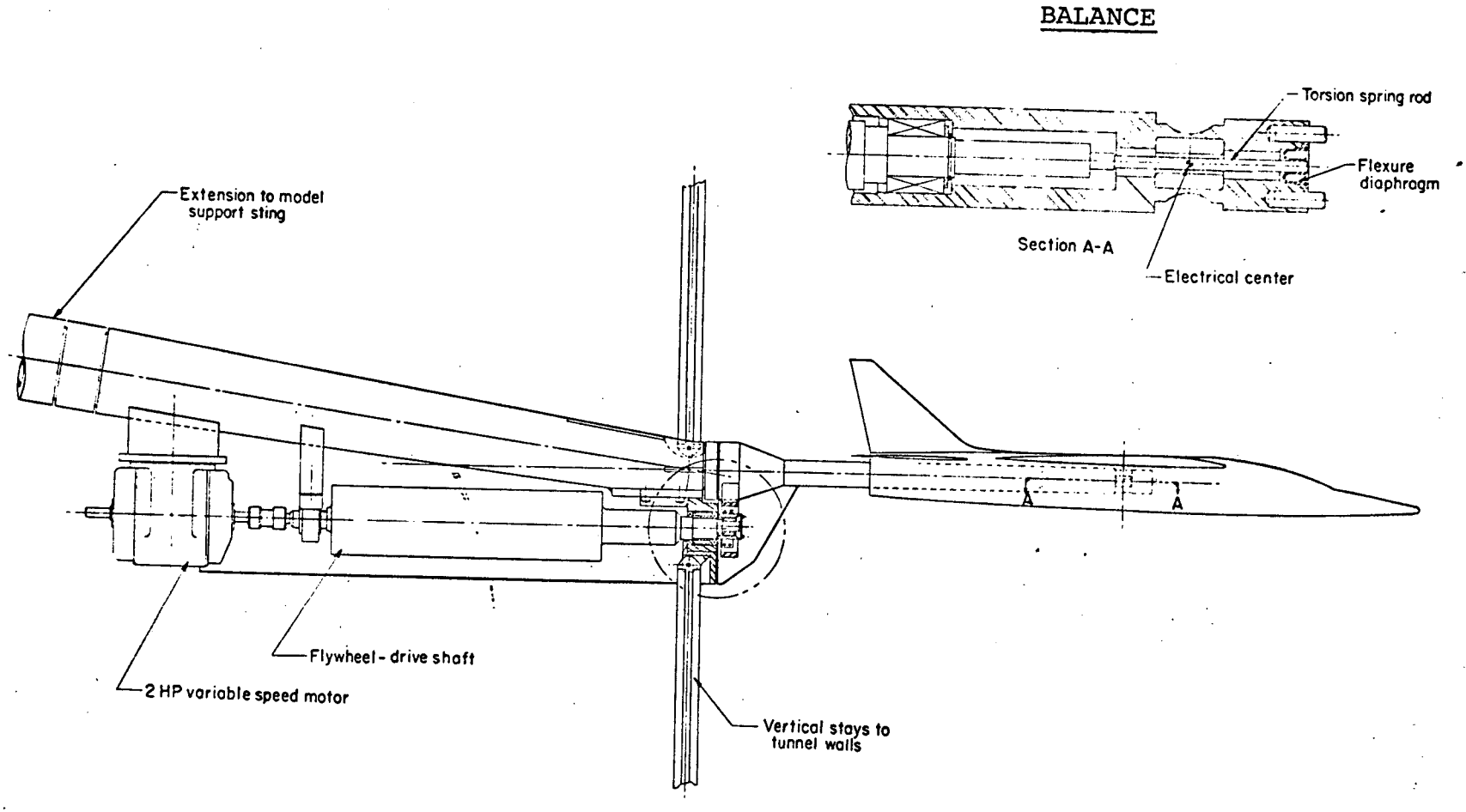

Fig. 3 Forced-oscillation roll apparatus
7x10 Foot High Speed Tunnel
8 Foot Transonic Pressure Tunnel
NASA - LRC

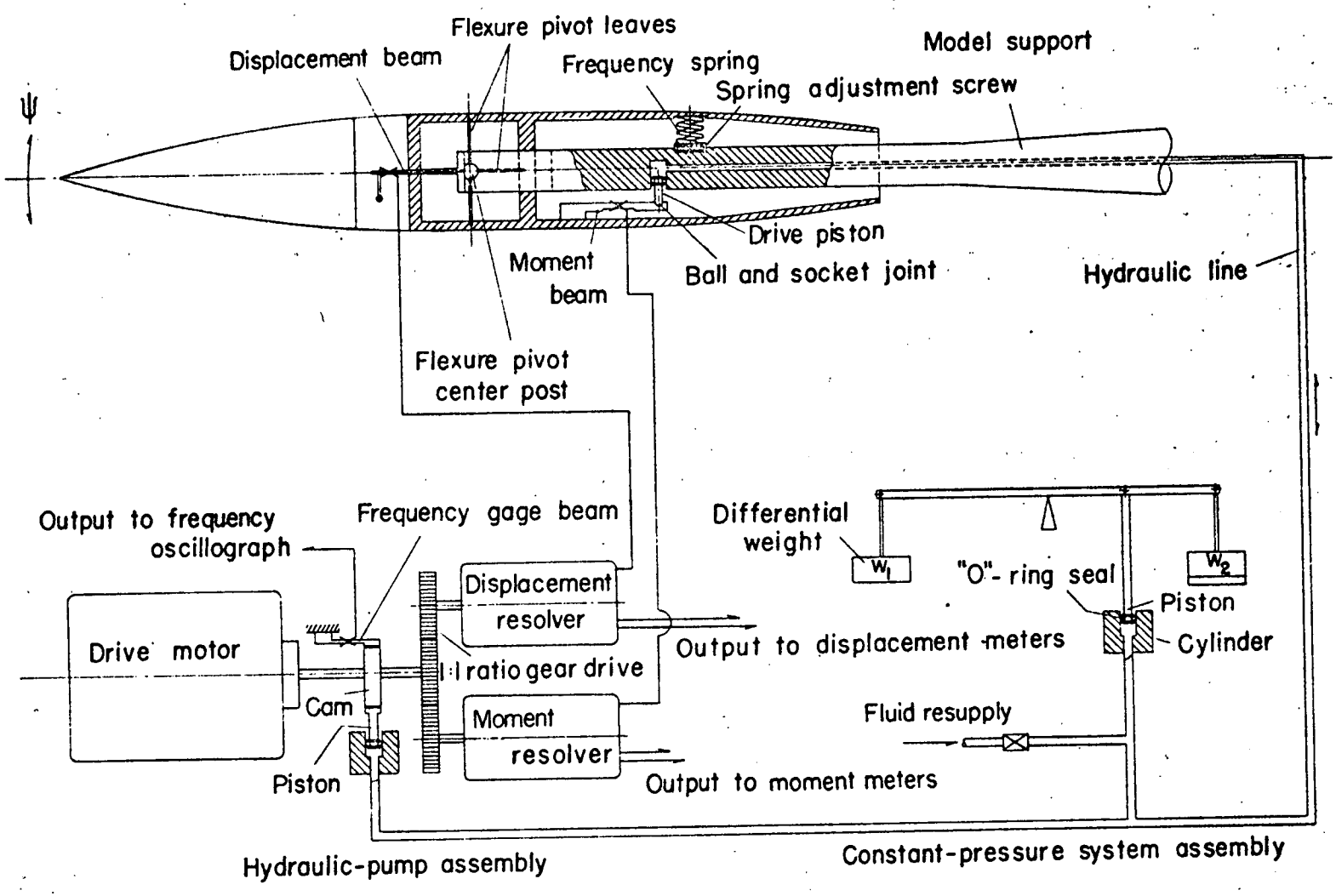

Fig. 4 Forced-oscillation pitch or yaw apparatus

NASA – LRC

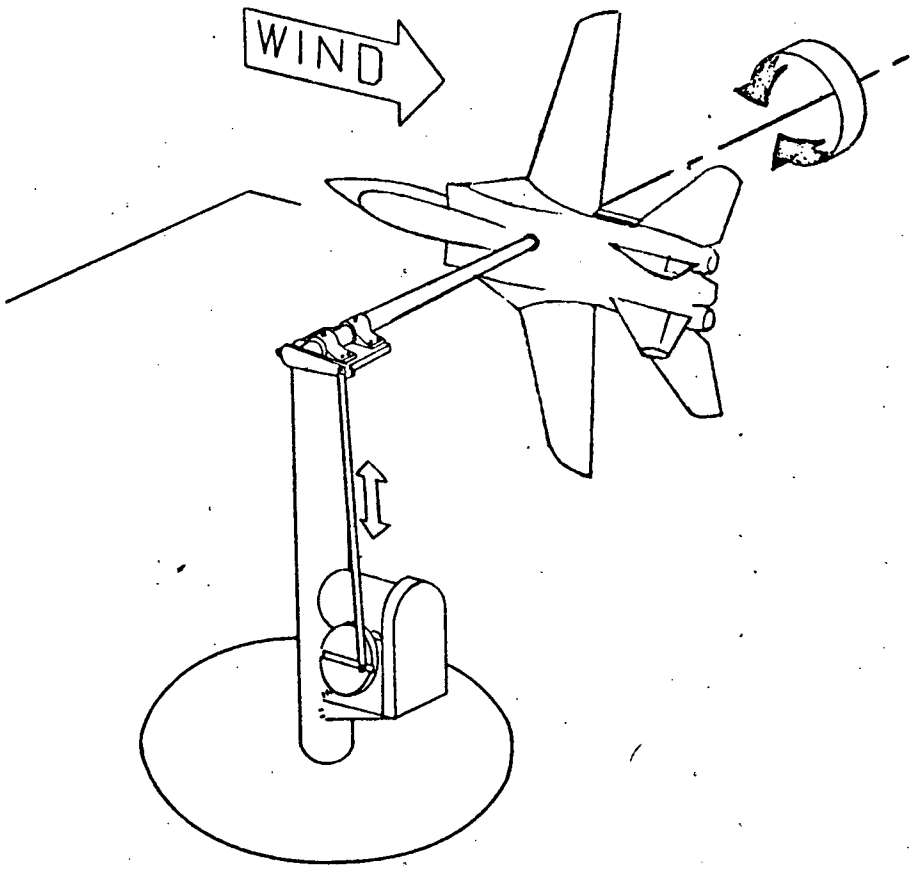

Fig. 5 Forced-Oscillation Pitch, Yaw or Roll Apparatus
(Yawing Setup)
Full Scale Tunnel
NASA LRC

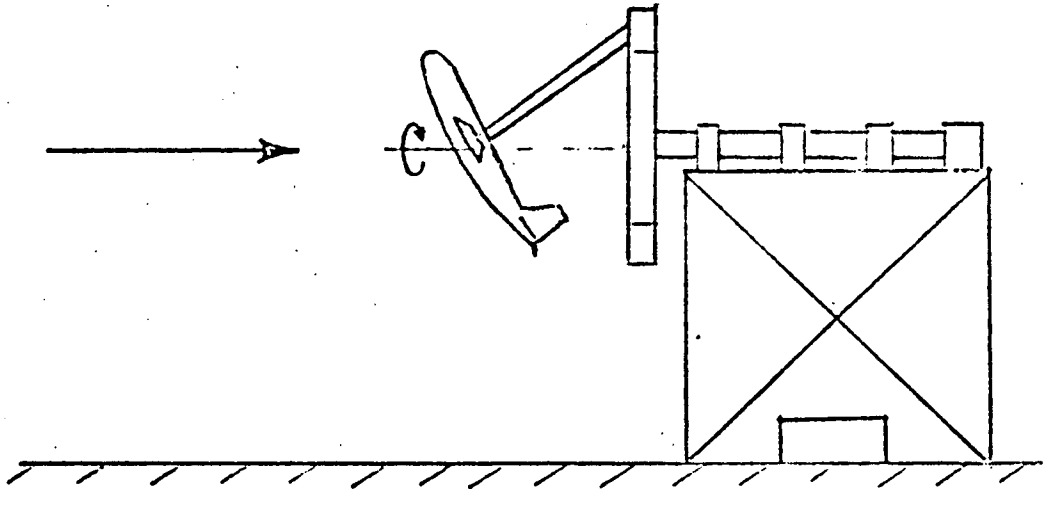

Fig. 6 Continuous rotation (rotary balance) apparatus
Full Scale Tunnel
NASA LRC

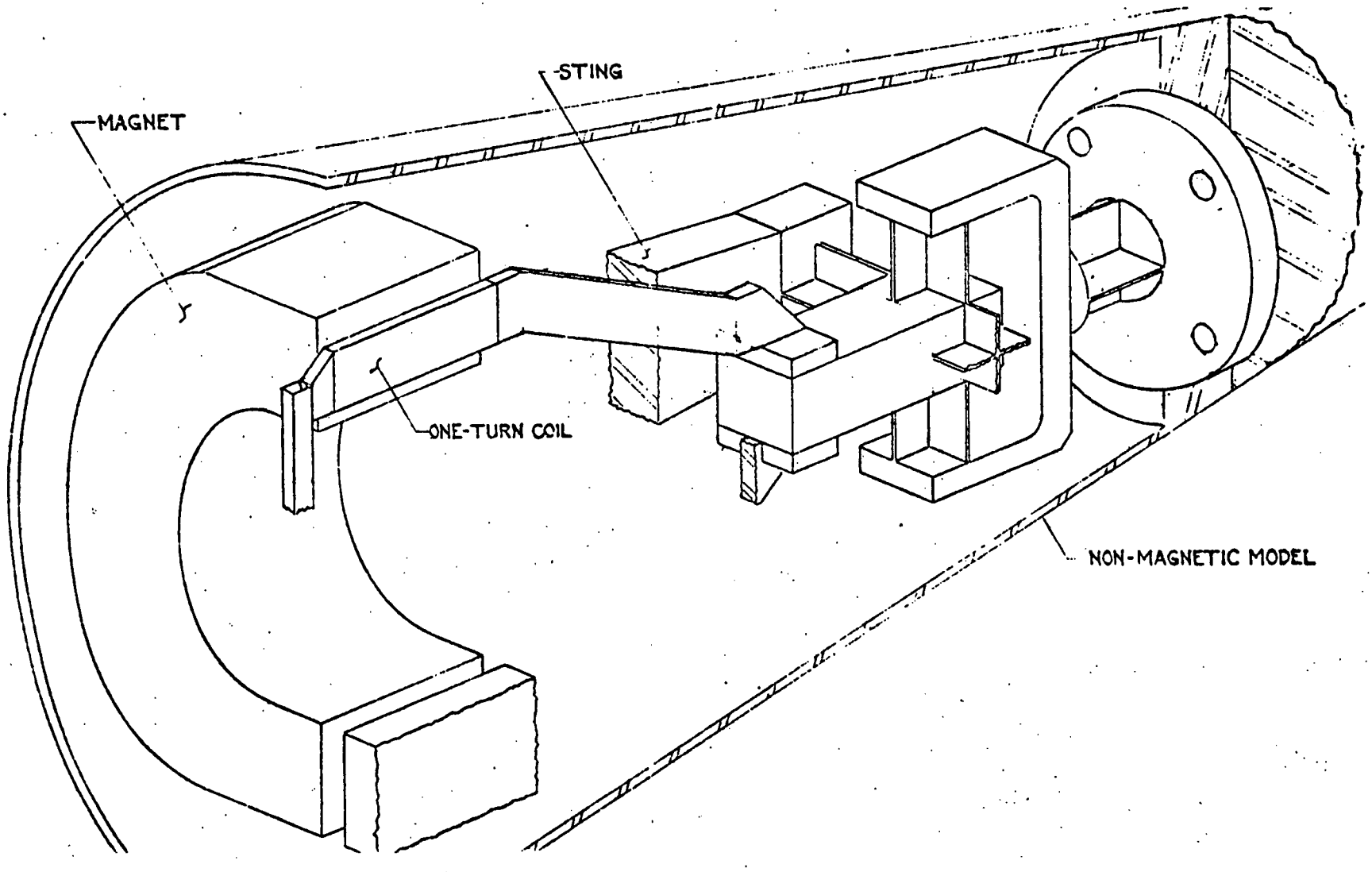

Fig. 7 Forced-oscillation cross-derivative apparatus
30 inch Wind Tunnel
NAE

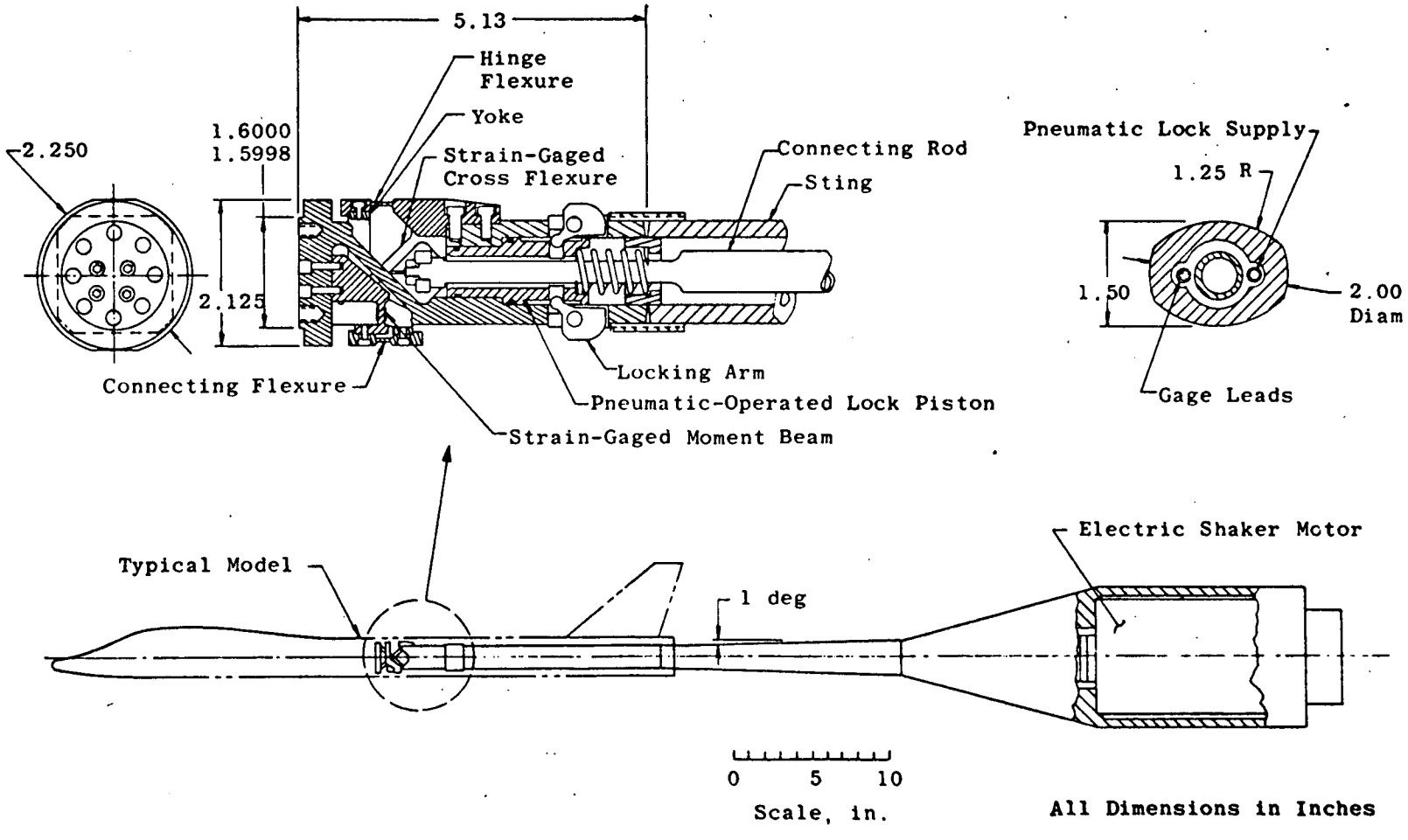

Fig. 8 Forced-oscillation pitch or yaw apparatus
Tunnels 4T, 16T, 16S, A, B, C
VKF and PWT

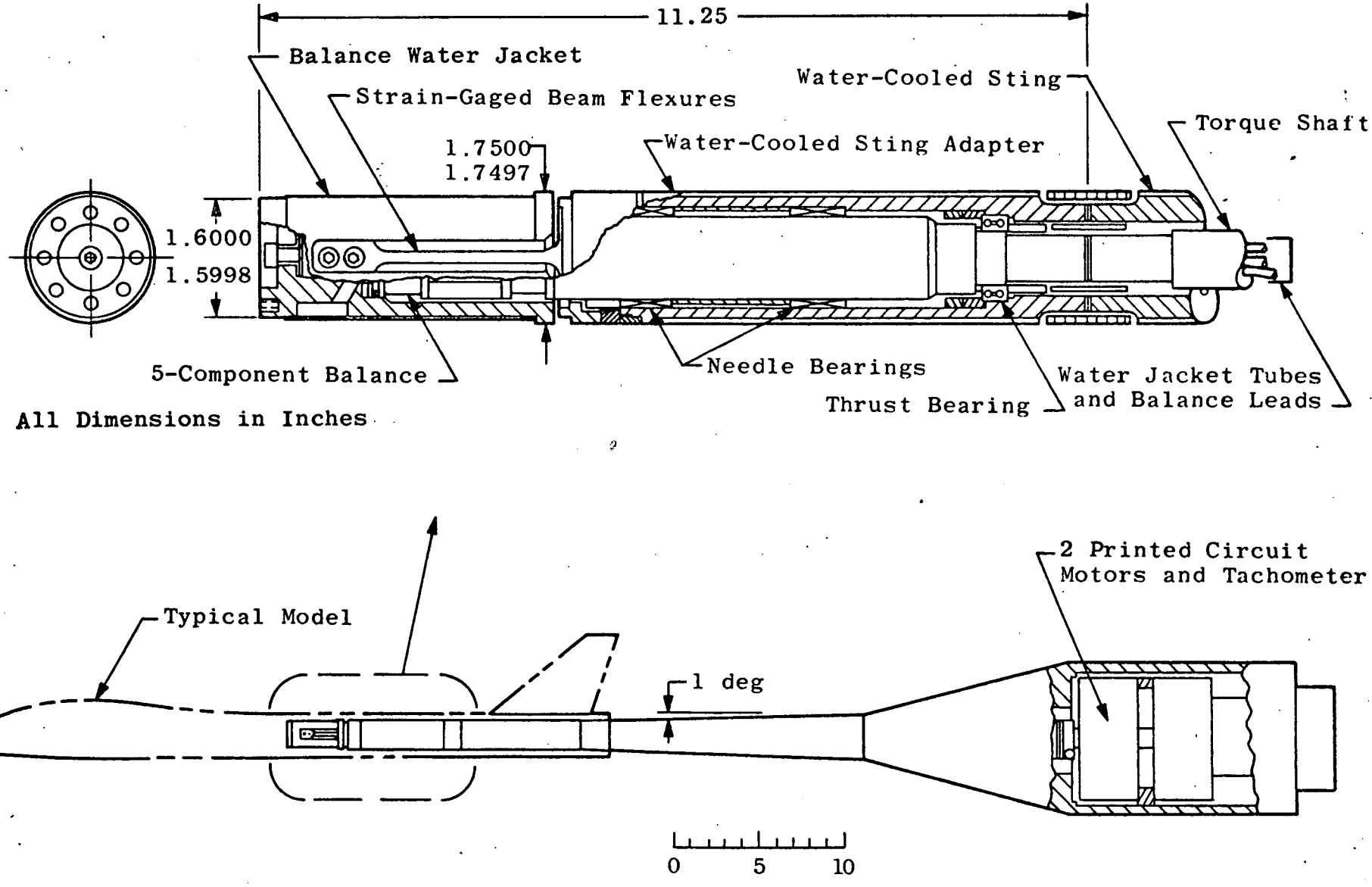

Fig. 9 Forced-oscillation roll apparatus
Tunnels 4T, 16T, 16S, A, B, C
VKF and PWT

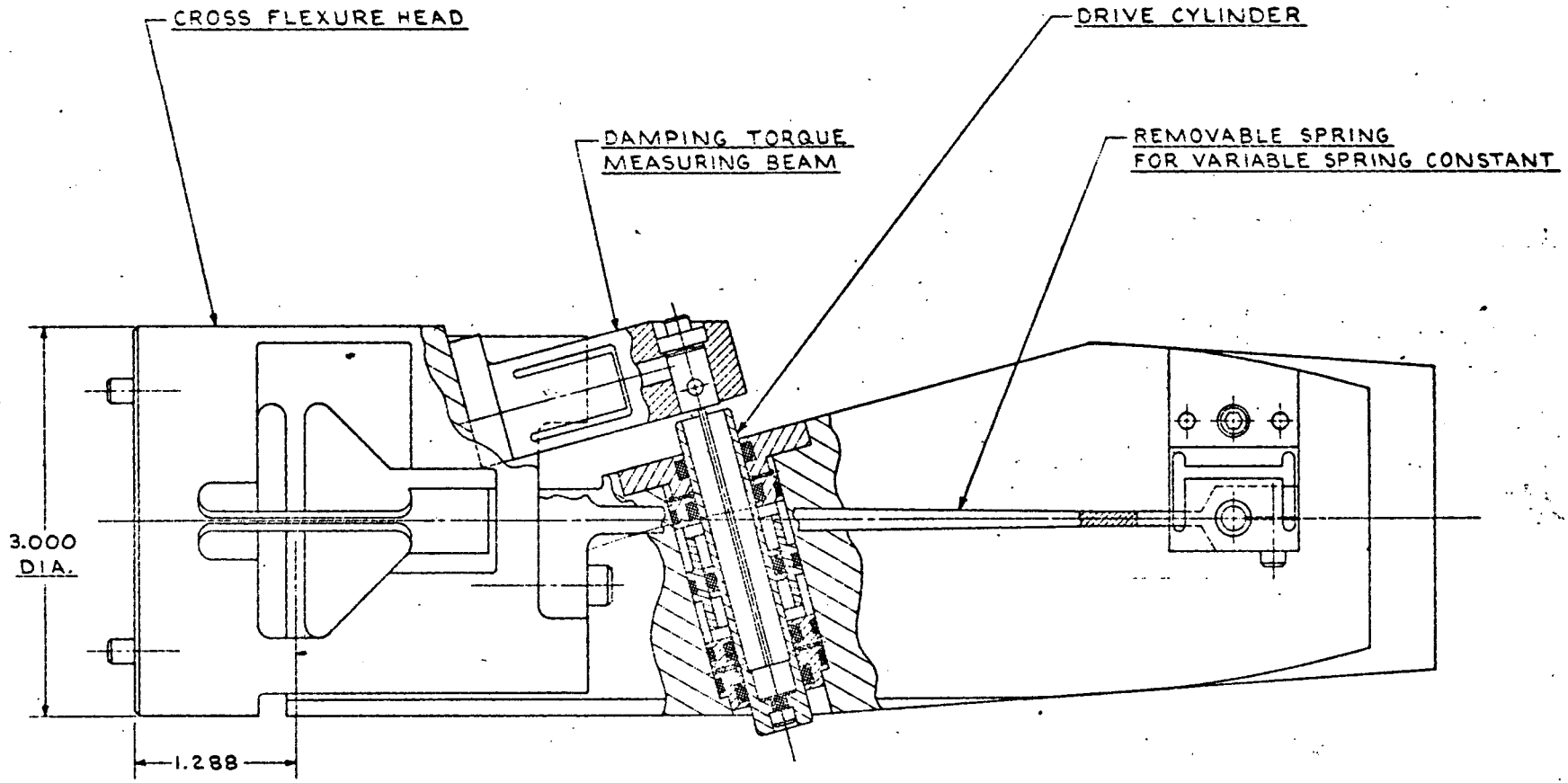

LOADS AND PARAMETERS		
ALLOWABLE LOADS	FORCING LOADS	ANGLES
600# N.F.	240. IN.#	OSCILLATING ± 3°
600# DRAG		ALLOWABLE P.M. ± 1°
150# S.F.		
300 IN.# Y.M.		f=1-30 Hz
177 IN.#/DEG. NO SPRINGS		
550 IN.#/DEG. WITH SPRINGS		

Fig.10 Forced-oscillation pitch apparatus
Tunnel 4T
PWT

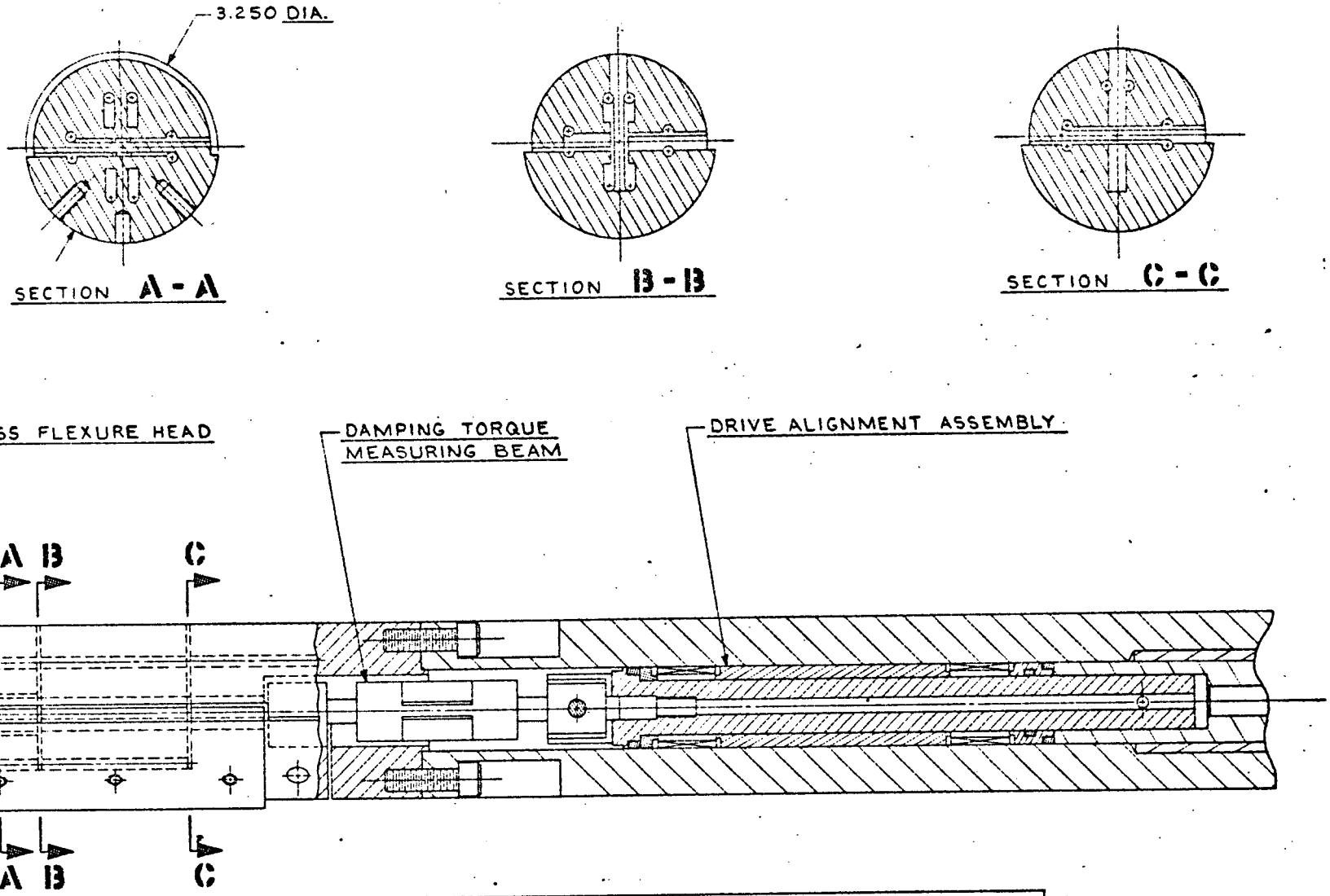

N. F. 4000 #	DRAG 800 #
P. M. 4000 IN. #	AMPLITUDE ± 2°
S. F. 1000 #	ROLL DAMPING 0-200 IN. #
Y. M. 1000 IN. #	SPRING CONSTANT 600 IN. #/DEG.

Fig. 11 Forced-oscillation roll apparatus (in design)
Tunnels 16T and 16S
PWT